

DTIC FILE COPY

(2)

SECURITY CLASSIFICATION OF THIS PAGE

REPORT DOCUMENTATION PAGE

1a. RESTRICTIVE MARKINGS UNCLASSIFIED		1b. RESTRICTIVE MARKINGS	
2a. SECURITY CLASSIFICATION AUTHORITY		3. DISTRIBUTION AVAILABILITY OF REPORT 1. <input type="checkbox"/> release; distribution unlimited.	
2b. DECLASSIFICATION/DOWNGRADING SCHEDULE			
4. PERFORMING ORGANIZATION REPORT NUMBER(S)		5. MONITORING ORGANIZATION REPORT NUMBER(S) AFOSR-TR- 88-1125	
6a. NAME OF PERFORMING ORGANIZATION Dr. Jacek Lagowski) Prof. H.C. Gatos) MIT	6b. OFFICE SYMBOL <i>(If applicable)</i> NE	7a. NAME OF MONITORING ORGANIZATION Air Force Office of Scientific Research	
6c. ADDRESS (City, State and ZIP Code) Massachusetts Institute of Technology 77 Massachusetts Ave. Cambridge, MA 02139		7b. ADDRESS (City, State and ZIP Code) Bolling Air Force Base, DC 20332	
8a. NAME OF FUNDING/SPONSORING ORGANIZATION AFOSR	8b. OFFICE SYMBOL <i>(If applicable)</i> NE	9. PROCUREMENT INSTRUMENT IDENTIFICATION NUMBER AFOSR-86-0342	
10. ADDRESS (City, State and ZIP Code) Bldg 410 Bolling AFB DC 20332-6448		10. SOURCE OF FUNDING NOS	
11. TITLE (Include Security Classification) Investigation of Defect & Electronic Interactions ASSOCIATED		PROGRAM ELEMENT NO.	PROJECT NO.
12. PERSONAL AUTHORIS WITH GAI AS DEFECT PROCESSING; Lagowski, Jacek and Gatos, Harry C.		TASK NO.	WORK UNIT NO.
13a. TYPE OF REPORT Annual	13b. TIME COVERED FROM 2/28/87 TO 2/29/88	14. DATE OF REPORT (Yr., Mo., Day) 1988 August 1	15. PAGE COUNT 37
16. SUPPLEMENTARY NOTATION			
17. COSATI CODES		18. SUBJECT TERMS (Continue on reverse if necessary and identify by block number)	
FIELD	GROUP	SUB GR.	
19. ABSTRACT (Continue on reverse if necessary and identify by block number) Our research in the period Feb. 28, 1987 to Feb. 29, 1988 resulted in five publications enclosed with this report and two completed Ph.D. theses. The research focussed on the properties of low diffusivity transition elements and their direct role (compensating levels) and indirect role (impurity gettering) in achieving semi-insulating III-V compounds. The results of our systematic study on optical and electronic properties of vanadium in GaAs were summarized in a detailed publication. A similar publication, dealing with properties of titanium, is under preparation. Our study established the positions of the energy levels of substitutional V and Ti (both donor and acceptor states) and concluded that they are not suitable for achieving semi-insulating GaAs. In InP, however, the deep Ti donor level (Ti^{4+}/Ti^{3+}) has an ideal location (0.63 eV below the conduction band) for producing a new type of semi-insulating InP based on codoping with Ti and shallow acceptors. In spite of wrong energy level positions, the vanadium was found to be beneficial for obtaining semi-insulating GaAs. It plays a more subtle chemical role as a gettering agent for shallow donor			
20. DISTRIBUTION/AVAILABILITY OF ABSTRACT UNCLASSIFIED/UNLIMITED <input type="checkbox"/> SAME AS RPT. <input type="checkbox"/> DTIC USERS <input type="checkbox"/>		21. ABSTRACT SECURITY CLASSIFICATION UNCLASSIFIED	
22a. NAME OF RESPONSIBLE INDIVIDUAL <i>J. H. Gatos</i>		22b. TELEPHONE NUMBER <i>(Include Area Code)</i> 202-767-4931	22c. OFFICE SYMBOL NE

**DTIC
SELECTED
S OCT 13 1988 E**

SECURITY CLASSIFICATION OF THIS PAGE

19. Abstract

impurities (Si and S) in the melt during the solidification process. Titanium on the other hand, was found to have no gettering effect with shallow donor impurities in GaAs. It was concluded that Ti doping is of no practical importance for producing semi-insulating GaAs.

In order to investigate the behavior of transition metal elements in ternary compounds we have developed a novel procedure for the growth of uniform ternary crystals based on liquid phase electroepitaxy (LPEE). In Ga_xAs ($x \approx 0.52$) and $\text{Al}_x\text{Ga}_{1-x}\text{As}$ with (x up to 0.4) were grown with this method. Doping with vanadium was realized, however, attempts to dope the crystals with Ti were unsuccessful, apparently due to gettering of Ti by carbon elements of the LPEE growth apparatus.

Investigation of native defects in GaAs concentrated on certain experimental aspects of the EL2 defect (this research was co-sponsored by NASA and Sumitomo Electric). Accordingly, we have developed a procedure which enabled the determination of the Fermi energy and the concentration and the occupancy of the EL2 level from high resolution optical measurements of the 1.039 eV zero phonon line. This procedure was subsequently employed for empirical unification of the EL2 properties and first quantitative correlation between various EL2 manifestations.

A detailed study of plastically deformed GaAs has identified the introduction of a deep acceptor defect as the major deformation-induced electronic level. EL2 concentration did not increase after deformation. Thus, the widely disputed enhancement of the EPR signal of the arsenic antisite As_{Ga} in deformed semi-insulating GaAs must have originated from the increased ionization of As_{Ga} rather than the generation of new antisite defects.

Accession For	
NTIS GRA&I	<input checked="" type="checkbox"/>
DTIC TAB	<input checked="" type="checkbox"/>
Unannounced	<input type="checkbox"/>
Justification	
By _____	
Distribution/	
Availability Codes	
Dist	Avail and/or Special
A-1	



SUMMARY

AFOSR-TR. 88-1125

Our research in the period February 28, 1987 to February 29, 1988, resulted in five publications enclosed with this report and two completed Ph.D. theses. The research focussed on properties of low diffusivity transition elements and their direct role (compensating levels) and indirect role (impurity gettering) in achieving semi-insulating III-V compounds. The results of our systematic study on optical and electronic properties of vanadium in GaAs were summarized in a detailed publication (Ref. 1). A similar publication, dealing with properties of titanium, is under preparation. Our study established the positions of the energy levels of substitutional V and Ti (both donor and acceptor states) and concluded that they are not suitable for achieving semi-insulating GaAs. In InP, however, the deep Ti donor level (Ti^{4+}/Ti^{3+}) has an ideal location (0.63 eV below the conduction band) for producing a new type of semi-insulating InP based on codoping with Ti and shallow acceptors (Ref. 2). In spite of wrong energy level positions, the vanadium was found to be beneficial for obtaining semi-insulating GaAs. It plays a more subtle chemical role as a gettering agent for shallow donor impurities (Si and S) in the melt during the solidification process (Ref. 3). Titanium, on the other hand, was found to have no gettering effect with shallow donor impurities in GaAs. It was concluded that Ti doping is of no practical importance for producing semi-insulating GaAs.

In order to investigate the behavior of transition metal elements in ternary compounds we have developed a novel procedure for the growth of uniform ternary crystals based on liquid phase electroepitaxy (LPEE). $In_xGa_{1-x}As$ ($x \approx 0.52$) and $Al_xGa_{1-x}As$ with (x up to 0.4) were grown with this method (Ref. 4). Doping with vanadium was realized, however, attempts to dope the crystals with Ti were unsuccessful apparently due to gettering of Ti by carbon elements

of the LPEE growth apparatus.

Investigation of native defects in GaAs concentrated on certain experimental aspects of the EL2 defect (this research was co-sponsored by NASA and Sumitomo Electric). Accordingly, we have developed a procedure which enabled the determination of the Fermi energy and the concentration and the occupancy of the EL2 level from high resolution optical measurements of the 1.039 eV zero phonon line (Ref. 5). This procedure was subsequently employed for empirical unification of the EL2 properties and first quantitative correlation between various EL2 manifestations (Ref. 6).

A detailed study of plastically deformed GaAs (Ref. 7) has identified the introduction of a deep acceptor defect as the major deformation-induced electronic level. EL2 concentration did not increase after deformation. Thus, the widely disputed enhancement of the EPR signal of the arsenic antisite As_{Ga} in deformed semi-insulating GaAs must have originated from the increased ionization of As_{Ga} rather than the generation of new antisite defects.

LIST OF PUBLICATIONS AND Ph.D. THESES
SUPPORTED BY AFOSR GRANT

1. A.M. Hennel, C.D. Brandt, K.Y. Ko, J. Lagowski, and H.C. Gatos
"Optical and electronic properties of vanadium in gallium arsenide,"
J. Appl. Phys. 62, 163 (1987).
2. C.D. Brandt, "A study of energy levels introduced by 3d transition elements in III-V compound semiconductors," Ph.D. Thesis, MIT, June 1987.
3. Kei Yu Ko, "Impurity gettering by transition elements in GaAs; growth of semi-insulating GaAs crystals," Ph.D. Thesis, MIT, February 1988.
4. T. Bryskiewicz, M. Bugajski, B. Bryskiewicz, J. Lagowski, and H.C. Gatos, "LPEE growth and characterization of $\text{In}_{1-x}\text{Ga}_x\text{As}$ bulk crystals," *Inst. Phys. Conf. Ser.* 91, 259 (1988).
5. J. Lagowski, M. Bugajski, M. Matsui, and H.C. Gatos, "Optical characterization of semi-insulating GaAs: Determination of the Fermi energy, the concentration of the midgap EL2 level and its occupancy," *Appl. Phys. Lett.* 51, 511 (1987).
6. J. Lagowski, M. Matsui, M. Bugajski, C.H. Kang, M. Skowronski, H.C. Gatos, M. Hoinkis, E.R. Weber and W. Walukiewicz, "Quantitative correlation between the EL2 midgap donor, the 1.039 eV zero phonon line, and the EPR arsenic antisite signal," *Inst. Phys. Conf. Ser.* 91, 137 (1988).
7. M. Skowronski, J. Lagowski, M. Milshtein, C.H. Kang, F.P. Dabkowski, A. Hennel and H.C. Gatos, "Effects of plastic deformation on electronic properties of GaAs," *J. Appl. Phys.* 62, 3791 (1987).

Optical and electronic properties of vanadium in gallium arsenide

A. M. Hennel,^{a)} C. D. Brandt, K. Y. Ko, J. Lagowski, and H. C. Gatos
Massachusetts Institute of Technology, Cambridge, Massachusetts 02139

(Received 15 January 1987; accepted for publication 10 March 1987)

The effects of vanadium doping on the electrical and optical properties of GaAs were systematically studied in melt-grown crystals prepared by the liquid-encapsulated Czochralski and horizontal Bridgman techniques and in epitaxial crystals prepared by liquid-phase electroepitaxy. By employing deep-level transient spectroscopy, Hall-effect measurements and the V^{2+} ($3d^3$) and V^{3+} ($3d^2$) intracenter optical-absorption spectra, one vanadium-related level was identified in all crystals, i.e., the substitutional-vanadium acceptor level (V^{3+}/V^{2+}) at 0.15 ± 0.01 eV below the bottom of the conduction band. From the absorption measurements we conclude that the vanadium (V^{4+}/V^{3+}) donor level must be located within the valence band. Because of its energy position, the above level cannot account for the reported semi-insulating properties of V-doped GaAs. We observed no midgap levels resulting from vanadium-impurity (defect) complexes. The high resistivity reported for certain V-doped GaAs crystals must result from indirect effects of vanadium, such as the gettering of shallow-level impurities.

I. INTRODUCTION

In the last few years several laboratories have reported the successful growth of semi-insulating (SI) V-doped GaAs, emphasizing its potential for improving device-processing characteristics relative to Cr-doped GaAs.¹ SI V-doped GaAs crystals have been grown by liquid-encapsulated Czochralski (LEC),²⁻⁵ vapor-phase epitaxy (VPE),⁶ and metallo-organic chemical vapor deposition (MOCVD)^{7,8} techniques. The growth of low-resistivity V-doped GaAs crystals by LEC^{9,10} and horizontal Bridgman (HB)^{5,11} techniques has also been reported. In the above studies the positions of the energy levels tentatively attributed to vanadium range from near the conduction band edge⁹⁻¹² to midgap.^{2,6,7}

It has also been shown^{13,14} that the diffusivity of vanadium in GaAs is about one order of magnitude lower than that of chromium. On the basis of this finding and the report of a level at $E_v + 0.58$ eV in V-doped VPE GaAs,⁶ a compensation mechanism for V-doped SI GaAs was proposed.^{13,14} These reports also concluded that V-doped SI GaAs would be superior in quality to all other commercially available types of SI GaAs crystals.

In this paper we discuss the effects of vanadium on the properties of GaAs based on the results of studies carried out on a series of V-doped melt- and solution-grown GaAs crystals using different growth and doping conditions. We show that the only vanadium-related level within the GaAs energy gap is an acceptor level at 0.15 eV below the conduction band. Some preliminary results have already been presented.¹⁵⁻¹⁷

II. EXPERIMENTAL PROCEDURES

Vanadium-doped melt-grown GaAs crystals were prepared by the LEC and HB techniques by using both pyrolytic boron nitride (PBN) and quartz crucibles. Two different

types of crucibles were used in order to test the hypothesis that inconsistencies in the reported data resulted from interactions of vanadium with impurities originating in the crucible. (For example, SI LEC GaAs crystals were grown by Wacker-Chemictronic with the use of quartz crucibles.^{4,13}) Doping with vanadium at concentrations reaching a level of $3 \times 10^{19} \text{ cm}^{-3}$ in the melt was realized by adding ultrapure elemental vanadium (99.9995%) or vanadium pentoxide V_2O_5 (99.995%) to the GaAs melt. The use of V_2O_5 was motivated by the speculation that vanadium-oxygen complexes could be responsible for deep levels in GaAs.^{6,7}

Some of the crystals were additionally doped with either shallow donors (Se, Si) or shallow acceptors (Zn) in order to vary the Fermi-level position across the entire band gap.

A key element in this study was the investigation of low-temperature solution-grown *n*-type V-doped crystals prepared by liquid-phase electroepitaxy (LPEE).¹⁸ Without intentional doping, this technique yields electron-trap-free GaAs crystals,¹⁹ providing a unique means for the unambiguous identification of levels introduced by vanadium.

In our investigation we also employed melt-grown inverted thermal conversion (ITC) V-doped GaAs crystals.²⁰ This new type of GaAs crystal contains virtually no native midgap levels (EL2), allowing the study of V-related optical-absorption spectra without interference from the well-known EL2 absorption.

Hall-effect measurements were conducted by using the standard Van der Pauw configuration. Ohmic contacts were fabricated by using an In/Sn alloy for *n*-type samples and an In/Zn alloy for *p*-type samples. Typically, measurements were carried out at 300 and 77 K. For several samples, carrier concentration as a function of temperature was measured over the range of 170–465 K.

The features of our transient capacitance system pertinent to this study include (a) precise temperature control and monitoring in the range 15–420 K, (b) direct emission-rate measurements over a range 10^{-3} – 10^4 s^{-1} from capacitance relaxation recorded with a signal averager, (c) stan-

^{a)} On leave from the Institute of Experimental Physics, Warsaw University, Warsaw, Poland.

dard deep-level transient spectroscopy (DLTS) mode operation with the use of a boxcar averager, and (d) optical deep-level spectroscopy (ODLTS) operation with the use of 1.06- μm excitation from a YAG laser. Schottky diodes were fabricated by evaporating Au onto *n*-type samples and Al onto *p*-type material.

Optical-absorption measurements were performed at 300, 77, and 5 K on a Cary model 17 spectrophotometer using a helium-gas-flow cryostat. Samples were typically from 0.5 to 1.0 cm thick. All of the absorption measurements performed at 5 K were preceded by a period of white light illumination in order to photoquench the well-known absorption due to EL2. All of the photoconductivity measurements were performed at 77 K on a simple LiF prism-based optical system.

III. EXPERIMENTAL RESULTS AND DISCUSSION

A. Hall-effect measurements

Doping with vanadium increased the resistivity of *n*-type GaAs and had no effect on the resistivity of *p*-type crystals. Standard Hall-effect measurements on low-resistivity *n*-type V-doped GaAs crystals yielded low-temperature free-electron mobility (μ) values that were systematically smaller than those obtained at room temperature. Typical results for crystals with free-electron concentrations (n) equal to a few times 10^{16} cm^{-3} were the following: $\mu = 2800-3100 \text{ cm}^2/\text{V s}$ at 77 K and $\mu = 3400-3700 \text{ cm}^2/\text{V s}$ at 300 K. These results, indicative of a high degree of ionized impurity scattering at low temperature due to the presence of vanadium, can be tentatively explained by assuming that vanadium acts as an acceptor in this material.

From systematic Hall-effect measurements as a function of temperature between 170 and 465 K, the free-carrier concentration (n) can be plotted as a function of reciprocal temperature, as shown in Fig. 1. From these data the energy (E_A) of a compensating vanadium level was found to be

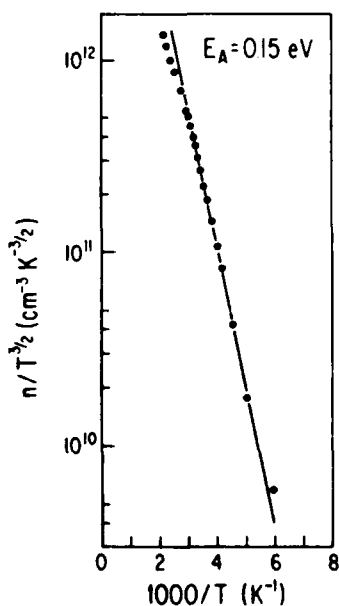


FIG. 1. Activation plot $n/T^{3/2}$ vs $1000/T$ of the free-electron concentration in high-resistivity LEC V-doped *n*-type GaAs ($N_V > N_D$).

0.15 ± 0.01 eV below the conduction band.¹⁶ In this analysis we have assumed the Hall-scattering factor (r_n) to be equal to 1.1 ($\pm 10\%$) throughout the measured temperature range.

Further analysis of the Hall data can provide an estimate of the concentration of vanadium centers by using the charge-balance expression given by Look²¹:

$$n + \frac{N_V}{1 + \Phi_{AC}/n} = N_D^+ - N_A^- ,$$

where $\Phi_{AC} = (g_{A0}/g_{A1})N_C' T^{3/2} e^{-E_A/kT}$ is a "modified" density-of-states function, $N_C' = 2(2\pi m_e^* k)^{3/2}/h^3 = 8.1 \times 10^{13} \text{ cm}^{-3} \text{ K}^{-3/2}$, N_V is the concentration of vanadium-related centers (assumed to be acceptors in this case), g_{A0} (g_{A1}) is the degeneracy of the unoccupied (occupied) state, E_A is the level energy measured from the bottom of the conduction band (a positive value), n is the concentration of free electrons, and N_D^+ and N_A^- are the concentrations of all ionized donors and acceptors (excluding vanadium), respectively. By curve fitting to the $n(T)$ data, the concentration of vanadium-related centers (N_V) can be estimated to be a few times 10^{16} cm^{-3} with an occupation fraction of these centers (N_V^-/N_V) between 0.4 and 0.6 at 200 K. With use of the free-electron mobility values in compensated GaAs calculated by Walukiewicz *et al.*^{22,23} for 77 and 300 K, the degree of shallow-donor compensation in these crystals (N_D^+/N_D) falls between 0.5 and 0.8. Combination of these results gives an upper limit for the concentration of vanadium-related acceptors of about $5 \times 10^{16} \text{ cm}^{-3}$.

B. DLTS measurements

DLTS and capacitance transient experiments were performed on low-resistivity GaAs:V,Se crystals where the selenium-donor concentration (N_D) exceeded the concentration of vanadium-related centers. The free-electron concentration in these crystals is weakly dependent on temperature, making it possible to carry out capacitance transient measurements to well below 77 K. Typical DLTS spectra in the range 100–440 K for a reference LEC GaAs:Se crystal, a LEC GaAs:V,Se crystal, a reference HB GaAs:Si crystal, and a HB GaAs:V,Se crystal are shown in Figs. 2(a), 2(b) and Figs. 3(a), 3(b), respectively. The dominant midgap level EL2 is clearly visible in all LEC and HB spectra at about 390 K. No other midgap levels could be detected. However, in V-doped crystals a new peak at about 100 K appears, indicating the presence of a new electron trap. In the *n*-type LPEE GaAs:V crystals this same electron trap is present, as shown in Fig. 2(c). These crystals are electron-trap free without vanadium doping; thus the presence of this new electron trap in this material provides proof that it is related to vanadium.

Capacitance transients caused by electron emission from this trap were measured as a function of temperature in order to obtain values of the activation energy and electron-capture cross section. From the thermal activation plot of the emission rate ($T^2 e_n^{-1}$ vs $1000/T$), which is presented in Fig. 4, we have found¹⁵ an activation energy for this vanadium-related trap of 0.15 ± 0.01 eV and an electron-capture cross section σ_∞ of about $2 \times 10^{-14} \text{ cm}^2$. We were unable to

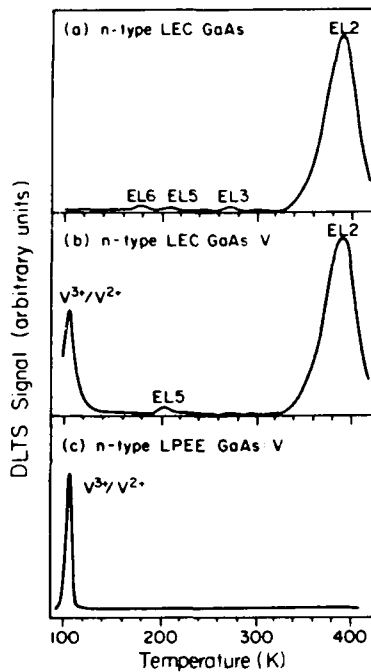


FIG. 2. DLTS spectra of (a) *n*-type LEC GaAs, (b) low-resistivity V-doped LEC GaAs ($N_V < N_D$), and (c) V-doped *n*-type LPEE GaAs. $t_1/t_2 = 5 \text{ ms}/10 \text{ ms}$.

measure the temperature dependence of this cross section. However, for the case of Ti-doped GaAs having an acceptor level of $E_c - 0.23 \text{ eV}$,²⁴ the activation energy of the electron-capture cross section was found to be smaller than 0.01 eV,

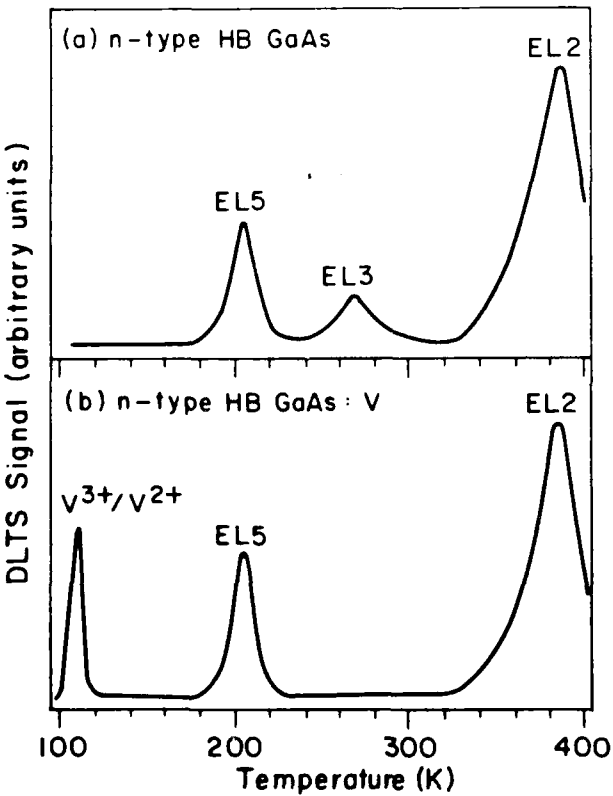


FIG. 3. DLTS spectra of (a) *n*-type HB GaAs and (b) low-resistivity V-doped HB GaAs ($N_V < N_D$). $t_1/t_2 = 5 \text{ ms}/10 \text{ ms}$.

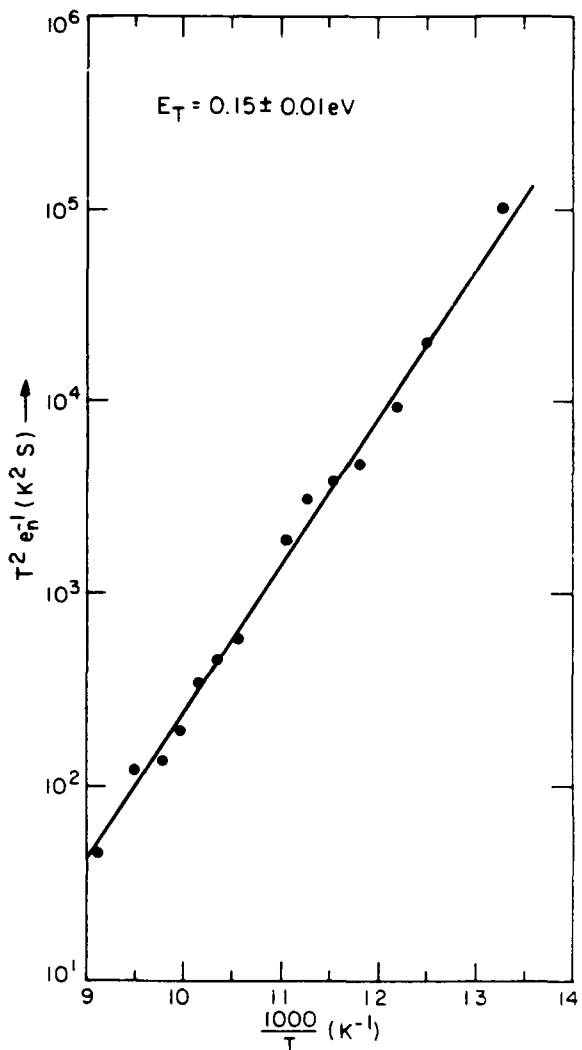


FIG. 4. Emission-rate thermal activation plot $T^2 e_n^-$ vs $1000/T$ for V-related electron trap in LEC GaAs.

i.e., our experimental error. Thus, taking into account the agreement between the DLTS and Hall-effect data concerning the level energy, we can assume that the activation energy for electron capture for vanadium is also negligible.

The concentration of vanadium centers calculated from the DLTS data was found to be approximately 10^{16} cm^{-3} , in agreement with the value obtained from Hall measurements.

DLTS measurements on *p*-type V-doped GaAs did not reveal any hole trap that could be related to vanadium. Typical DLTS spectra in the range 100–440 K for a reference HB GaAs:Zn crystal and a HB GaAs:V,Zn crystal are shown in Figs. 5(a) and 5(b), respectively. In addition, optical DLTS measurements on *n*-type crystals did not show any minority carrier traps that could be related to vanadium.

In view of the results presented thus far, several conclusions regarding the behavior of vanadium in GaAs can be drawn. Regardless of the dopant form (V or V_2O_5), crucible material (SiO_2 or PBN), or growth technique (LEC, HB, or LPEE), vanadium introduces one electron trap into the en-

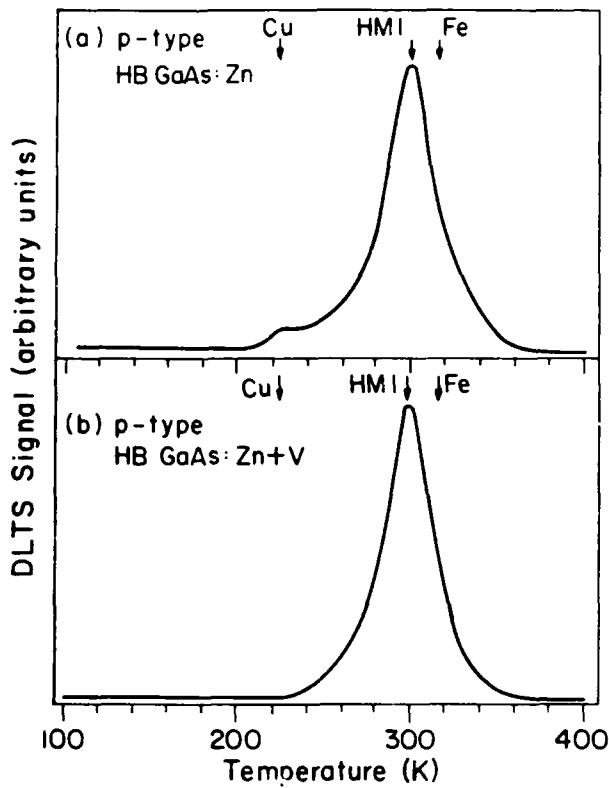


FIG. 5. DLTS spectra of (a) *p*-type HB GaAs and (b) V-doped HB GaAs. $t_1/t_2 = 5 \text{ ms}/10 \text{ ms}$.

ergy gap at 0.15 eV below the bottom of the conduction band. No evidence of any midgap level related to vanadium was found, which directly draws into question the utility of vanadium in producing semi-insulating GaAs. The identification of this 0.15-eV vanadium level as an acceptor will be more fully discussed in the following section.

It should be noted that results obtained in some other laboratories did indicate the presence of a vanadium-related acceptor level in the vicinity of the conduction band edge. Thus Clerjaud *et al.*¹² reported electron traps at $E_c - 0.14$ eV and $E_c - 0.23$ eV from DLTS measurements of HB GaAs:V, while Ulrici *et al.*¹⁰ reported an acceptor level in LEC GaAs:V at $E_c - 0.14$ eV. We think that the levels reported at $E_c - 0.14$ eV are undoubtedly related to vanadium, with the difference between our results and those quoted above lying within the experimental error.

C. Absorption and photoconductivity spectra

Having identified the level at $E_c - 0.15$ eV as being introduced by vanadium, we employed optical measurements to obtain information concerning its microscopic nature.

Optical-absorption measurements were performed on both *n*- and *p*-type, V-doped GaAs crystals. In this way, spectra were obtained for Fermi-level positions spanning the entire energy gap. The absorption spectra obtained fell into two primary groups:

(a) For all high-resistivity GaAs:V crystals and *p*-type GaAs:V, Zn crystals (independent of the zinc-doping level),

a characteristic double-peak absorption band was observed between 1.0 and 1.2 eV, preceded at 5 K by a weak zero-phonon line (ZPL) at 1.008 eV and a single absorption line at 0.909 eV. An additional absorption band starting at about 1.35 eV and superimposed on the fundamental absorption edge was also observed. All of these absorption features are shown in Fig. 6(a).

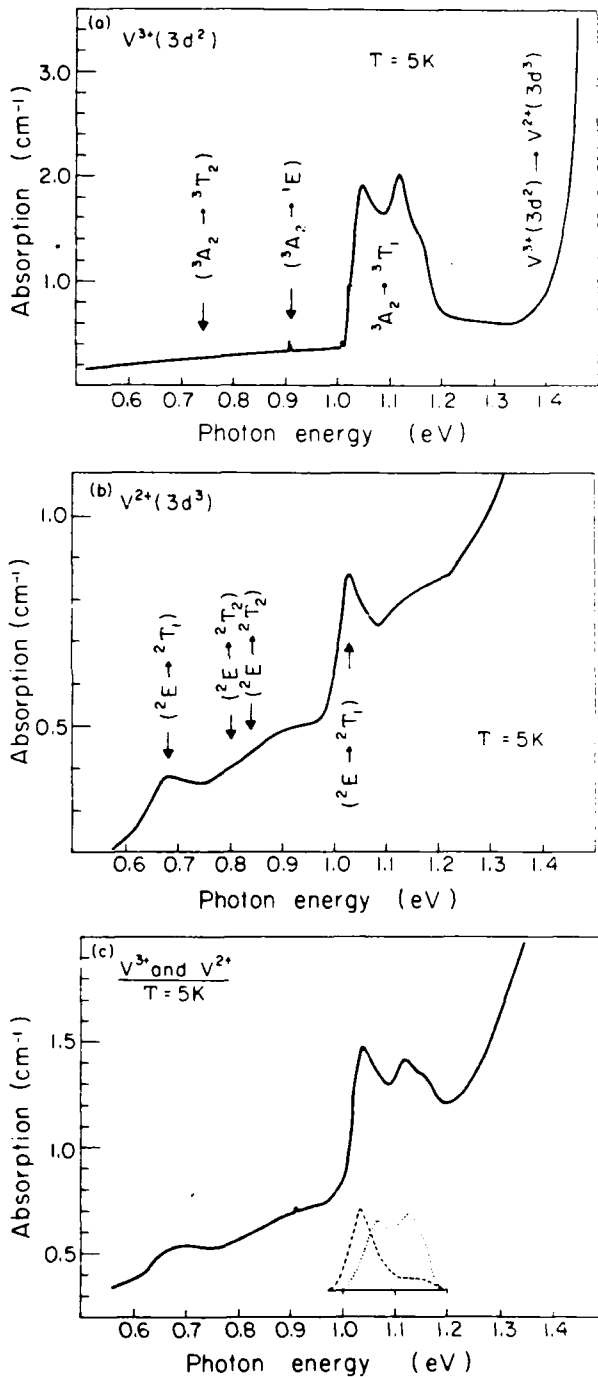


FIG. 6. Optical-absorption spectra of (a) *p*-type and high-resistivity, (b) *n*-type ($N_v < N_D$), and (c) *n*-type ($N_v > N_D$) V-doped GaAs obtained at 5 K. In (a) and (b) assignments of vanadium intracenter transitions according to Ref. 25 are indicated. The inset of (c) shows the relative contribution of the V^{2+} and V^{3+} charge states.

(b) For *n*-type GaAs:V,Se, heavily doped with selenium ($N_D > 10^{17} \text{ cm}^{-3}$), two absorption bands at 0.68 eV and 1.03 eV without any ZPL were observed, as shown in Fig. 6(b). These bands are superimposed on an absorption background that begins at about 0.3 eV.

For lightly doped *n*-type GaAs:V crystals, a mixed absorption spectrum, composed of both (a) and (b)-type absorption features, was observed. Figure 6(c) shows an example of such a mixed absorption spectrum.

The nature of the characteristic absorption band shown in Fig. 6(a) has already been studied and is discussed in detail in the review paper by Clerjaud.¹ This band constitutes an intracenter transition within neutral, substitutional [V³⁺(3d²)] vanadium between the ground ³A₂ and the excited ³T₁ state. Furthermore, the luminescence spectrum¹ (ZPLs at 0.74 eV), involving the excited ³T₂ and ground ³A₂ states of this V³⁺(3d²) configuration, was also observed in these same samples.²⁶ Therefore, the vanadium in all of our *p*-type and high-resistivity *n*-type crystals is in the neutral V³⁺(3d²) charge state. This assignment is further supported by the results of Clerjaud *et al.*¹² who correlated observation of the EPR spectrum of the neutral V³⁺(3d²) with the absorption spectrum in Fig. 6(a).

The absorption line at 0.909 eV in Fig. 6(a) has also been observed by Clerjaud *et al.*¹² and recently interpreted by Caldas *et al.*²⁵ as being due to the ³A₂ → ¹E spin-forbidden transition of the V³⁺(3d²) charge state.

Figure 6(a) also shows an absorption band starting at 1.35 eV whose intensity correlated with that of the main V³⁺ intracenter absorption. This result is in agreement with the existing assignment^{10,12} of this absorption to the optical transition:

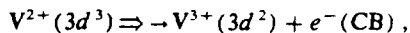


The second type of absorption spectrum shown in Fig. 6(b) is, in our opinion, due to intracenter transitions of the singly ionized V²⁺(3d³) charge state. This spectrum is observed in all low-resistivity *n*-type GaAs:V crystals, and its intensity follows that of the DLTS vanadium peak. Furthermore, Fig. 6(c) illustrates the smooth transition between the two different vanadium spectra when the Fermi level is located at the $E_c - 0.15$ eV vanadium level. The band at 1.03 eV had been observed by Clerjaud *et al.*¹² and interpreted in terms of the V²⁺(3d³) intracenter transition. However, they did not observe the band at 0.68 eV because of a rising low-energy absorption background. Ulrich *et al.*¹⁰ did observe both of these bands, but did not interpret them as being connected with the V²⁺(3d³) charge state or correlate them together. We can explain the reason for this omission as the observation by Ulrich *et al.* of a mixed V³⁺ and V²⁺ absorption spectrum similar to that presented in Fig. 6(c).

At this time we are unable to make a definite identification of the V²⁺(3d³) electron states responsible for the absorption bands presented in Fig. 6(b), because with the lack of a positive identification of any V²⁺ EPR spectra, the ground-state symmetry remains uncertain. However, Katayama-Yoshida and Zunger²⁷ and also Caldas *et al.*²⁵ have predicted that the ground state of the V²⁺(3d³) configuration in GaAs crystals should be the low-spin ²E state, rather

than the normally expected (according to Hund's rule) high-spin ⁴T₁ state. Within this model Caldas *et al.* have interpreted the entire V²⁺(3d³) absorption spectrum, as indicated in Fig. 6(b).

From our identification one can further conclude that the absorption background observed in Figs. 6(b) and 6(c) probably corresponds to the transition



which is complementary to the 1.35-eV absorption observed in the V³⁺ spectrum.

The results of photoconductivity measurements on these low-resistivity *n*-type samples are shown in Fig. 7. The presence of the same two maxima of the V²⁺(3d³) charge state at 0.68 and 1.03 eV in the photoconductivity spectrum is a well-known property of excited states of a many-electron impurity. These states are therefore degenerate with the GaAs conduction band and undergo an autoionization effect,^{1,28} making them observable under these experimental conditions.

All of the aforementioned assignments are further supported by electron-paramagnetic-resonance (EPR) measurements of our samples.²⁹ The characteristic substitutional V³⁺(3d²) spectrum⁴ was observed for all *p*-type and high-resistivity *n*-type V-doped GaAs samples. In the case of samples with the Fermi-level position above the $E_c - 0.15$ eV level, no EPR spectrum was found, which can be attributed to the high conductivity of such samples.

To conclude this discussion, we can state unequivocally that the optical and electrical properties of V-doped GaAs are self-consistent. Identification of the substitutional non-complexed-vanadium optical spectra enables us to identify the $E_c - 0.15$ eV level as the V³⁺(3d²)/V²⁺(3d³) single acceptor. Furthermore, the observation of the intracenter

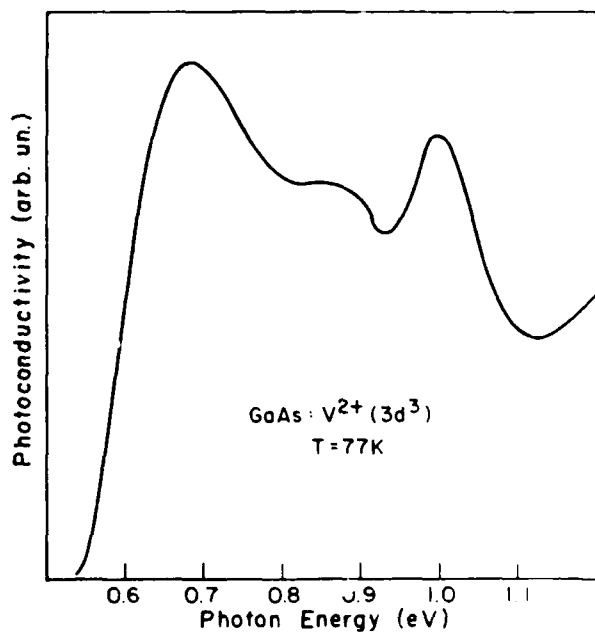


FIG. 7. Photoconductivity spectrum of *n*-type V-doped GaAs obtained at 77 K.

V^{3+} absorption spectrum for all positions of the Fermi level between the V^{3+}/V^{2+} acceptor level and the valence band proves that there is no other substitutional-vanadium level within the GaAs energy gap, i.e., that the $V^{4+}(3d^1)/V^{3+}(3d^2)$ donor level must be located within the valence band. Figure 8 schematically presents all of the substitutional-vanadium levels in GaAs.

D. Calibration of the optical spectra

The DLTS and optical-absorption spectra obtained from low-resistivity V-doped GaAs samples provide the data necessary to calculate the optical-absorption cross sections (σ) of the $V^{2+}(3d^3)$ intracenter transitions [Fig. 6(b)]. At liquid-helium temperature their values are the following:

$$\begin{aligned}\sigma(1.03 \text{ eV}) &= \frac{\alpha(1.03 \text{ eV}) - \alpha(0.95 \text{ eV})}{N(\text{DLTS})} \\ &= 3.5 \times 10^{-17} \text{ cm}^2 (\pm 20\%), \\ \sigma(0.68 \text{ eV}) &= \frac{\alpha(0.68 \text{ eV}) - \alpha(0.60 \text{ eV})}{N(\text{DLTS})} \\ &= 1.5 \times 10^{-17} \text{ cm}^2 (\pm 20\%),\end{aligned}$$

where $\alpha(E)$ is the absorption coefficient for the photon energy E , and $N(\text{DLTS})$ is the concentration of vanadium centers obtained from DLTS measurements.

Our as-grown LEC GaAs crystal have a native defect acting as a deep acceptor, which disappears after a standard 850 °C anneal.³⁰ This native defect provides compensation in as-grown material sufficient to position the Fermi level at or slightly below the 0.15-eV vanadium level, resulting in a V^{3+} or mixed absorption spectrum; after annealing, only a pure V^{2+} spectrum is observed. We have used this phenomenon to extend our calibration to the $V^{1+}(3d^2)$ main intracenter transition. Comparing the as-grown and annealed spectra of the same *n*-type V-doped samples, we were able to use the above calibration to find the $V^{1+}(3d^2)$ absorption cross section at liquid-helium temperature as

$$\begin{aligned}\sigma(1.04 \text{ eV}) &= \frac{\alpha(1.04 \text{ eV}) - \alpha(0.97 \text{ eV})}{N(\text{DLTS})} \\ &= 1 \times 10^{-16} \text{ cm}^2 (\pm 40\%).\end{aligned}$$

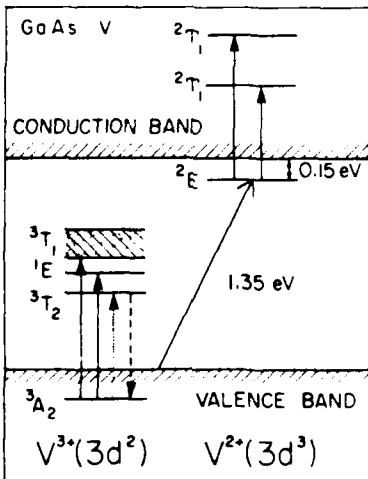


FIG. 8. Energy levels of the $V^{3+}(3d^2)$ and $V^{2+}(3d^3)$ charge states in GaAs. Vertical arrows represent intracenter transitions and the slanted arrow represents the charge transfer $V^{3+}(3d^2) + e^- \Rightarrow V^{2+}(3d^3)$. The indicated level symmetries have been taken from Ref. 25.

E. Theoretical considerations and comparison with other III-V compounds

In addition to all of the technological and experimental studies of V-doped GaAs, some theoretical calculations have also been performed.^{25,27} These calculations were not only directed toward an identification of a vanadium spin state (as was mentioned before), but also strove to provide positions of the energy levels within the band gap. The V^{3+}/V^{2+} acceptor level has been calculated to be at $E_c + 1.35 \text{ eV}$ (Ref. 25) and $E_c + 1.34 \text{ eV}$ (Ref. 27), respectively. The V^{4+}/V^{3+} donor level in both cases has been predicted to be inside the valence band; in one case its position could be estimated as -0.03 eV (Ref. 25) below the top of the valence band. All of these predictions are in a very good agreement with our experimental findings.

Furthermore, based on the findings of Ledebot and Ridley³¹ and also of Caldas *et al.*³² that the vacuum-referred binding energies (VRPE) of transition-metal impurities remain nearly constant within a given class of semiconducting compounds (i.e., III-V crystals), we can present the available data about substitutional-vanadium levels in the III-V semiconductors. In the case of indium phosphide, the $V^{4+}(3d^1)/V^{3+}(3d^2)$ donor level has been found at $E_v + 0.21 \text{ eV}$ (Refs. 33 and 34) or $E_v + 0.24 \text{ eV}$ (Ref. 35), and the $V^{3+}(3d^2)/V^{2+}(3d^3)$ acceptor level is proposed by Lambert *et al.*³⁶ to lie in the conduction band. For *n*-type gallium phosphide, the vanadium-acceptor level has only recently been identified at $E_c - 0.58 \text{ eV}$ (Ref. 37). Measurements on *p*-type GaP should reveal the vanadium-donor level as well.

All of these experimental results are presented in Fig. 9 with the use of the electron-affinity data from Ref. 32. One

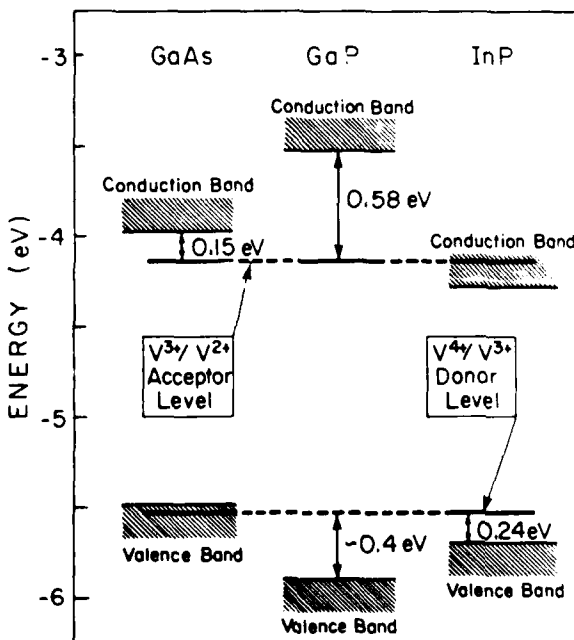


FIG. 9. Vacuum-related binding energies of the vanadium-donor and acceptor levels in some III-V compounds. The vanadium-donor level in GaP has not yet been observed, but is predicted to lie at $E_c + 0.4 \text{ eV}$.

can see excellent agreement between the reported vanadium VRBES and also predict that the vanadium-donor levels are located at about $E_c + 0.4$ eV in GaP and very close to the top of the valence band in GaAs.

It is also evident from this figure that none of the substitutional-vanadium levels in GaAs or InP can act as centers for producing SI material.

F. Implications for SI GaAs

All of the above experimental and theoretical results prove that the substitutional $V^{3+}/(3d^2)/V^{2+}(3d^3)$ acceptor level at $E_c - 0.15$ eV is the only vanadium-related level found within the GaAs energy gap. However, several authors have suggested the existence of electrically active vanadium-related complexes in GaAs^{5-8,10,37-39} as possibly providing a midgap level. Models invoking a vanadium-oxygen complex^{6,7} or a vanadium-arsenic vacancy complex^{10,38} have been put forth. We did not detect any optical or electronic evidence of a vanadium-related midgap level in our *n*-type LEC, HB, and LPPE V-doped crystals.

For the case of a vanadium-arsenic vacancy complex model,^{10,38} it should be mentioned that although an analogy with a chromium trigonal center $Cr^{2+}-X$ (see, for example, Ref. 1) is used, there is no experimental evidence (analogous to the known properties of the chromium complex) that such a vanadium complex exists. There is also no definite proof that the acoustic-paramagnetic-resonance (APR) spectra³⁸ and the thermally detected electron-paramagnetic-resonance (TDEPR) spectra³⁹ are vanadium related. The reported crystals contain several other transition-metal impurities, and the APR and TDEPR measurements give no information about the concentration of investigated anisotropic centers. Last, the authors of this model¹⁰ failed to grow any SI V-doped material.

During the course of our study, several HB SI V-doped crystals were successfully grown and characterized. We have found, however, that the Fermi-level position in these crystals is controlled by the deep donor EL2, which is present in concentrations greater than that of substitutional vanadium as determined from optical-absorption measurements. Furthermore, the absorption and EPR data from these SI samples are identical to those discussed in Sec. C.

All of these arguments lead quite clearly to the conclusion that vanadium does not play an electronic role in the formulation of SI GaAs. The results do suggest, however, that vanadium could play a more subtle chemical role (e.g., as a gettering agent), thus aiding in the growth of normal EL2-compensated SI material, rather than being directly responsible for its electrical properties. In Table I we have collected all of the published data on the energy levels in V-doped GaAs crystals as of this writing. Comments as to the actual origin of the dominant deep level in each case (e.g., V^{3+}/V^{2+} or EL2), in view of the results presented in this study, are also included.

IV. CONCLUSIONS

Through the use of DLTS, Hall-effect, and optical-absorption measurements, we have identified the substitutional-vanadium V^{3+}/V^{2+} acceptor level in GaAs at 0.15 eV

TABLE I. Deep levels observed in V-doped GaAs.

Energy position (eV)	Crystal growth method*	Relation to vanadium	Possible origin
$E_c - 0.15^b$	LEC, HB, LPPE	V^{3+}/V^{2+} acceptor	
$E_c - 0.14^c$	LEC	V^{3+}/V^{2+} acceptor	
$E_c - 0.14^d$	HB	V^{3+}/V^{2+} acceptor	
$E_c - 0.22^e$	LEC	not related to V	EL14 or Ti ^f
$E_c - 0.23^d$	HB	not related to V	EL14 or Ti ^f
$E_c - 0.5^g$	MOCVD	not related to V	?
$E_c - 0.77^h$	LEC	not related to V	EL2
$E_c + 0.58^i$	VPE	not related to V	HM1 ^j

* (LEC) liquid-encapsulated Czochralski, (HB) horizontal Bridgeman, (LPPE) liquid-phase electroepitaxy, (MOCVD) metallo-organic chemical vapor deposition, (VPE) vapor-phase epitaxy.

^b References 15, 16, and this study.

^c Reference 10.

^d References 11, 12, and 40.

^e Reference 9.

^f Reference 24.

^g Reference 7.

^h References 2 and 3.

ⁱ Reference 6.

^j J. Lagowski, D. G. Lin, T.-P. Chen, M. Skowronski, and H. C. Gates, *Appl. Phys. Lett.* **47**, 929 (1985).

^k J. Osaka, H. Okamoto, and K. Kobayashi, in *Semi-Insulating III-V Materials, Hakone, 1986*, edited by H. Kukimoto and S. Miyazawa (North-Holland/OHMSHA, Tokyo, 1986), p. 421.

below the bottom of the conduction band. The substitutional-vanadium V^{3+}/V^{2+} donor level was found to be located within the valence band. In addition, no evidence of any midgap level due to vanadium-impurity (defect) complexes was observed. These results confirm the fact that vanadium cannot provide the compensation necessary for producing SI GaAs. The high resistivity of some SI V-doped GaAs crystals can be readily explained by the overwhelming presence of the native defect EL2. We believe that vanadium can, however, play an important chemical role by removing or reacting with residual shallow donors during the growth of high-resistivity material.

ACKNOWLEDGMENTS

We are deeply indebted to Dr. T. Bryskiewicz for growing the V-doped LPPE GaAs crystals. We are very grateful to Dr. B. Clerjaud (Université Paris VI) for the EPR measurements of our crystals and many helpful discussions, to Dr. P. W. Yu for the luminescence measurements of our crystals, to Dr. P. Becla for his help in our photoconductivity measurements, and to L. Pawlowicz and F. Dabkowski for growing some of the V-doped LEC GaAs crystals used in this study. We are also grateful to the Air Force Office of Scientific Research and the Office of Naval Research for financial support and the IBM Corporation for C. D. Brandt's graduate fellowship.

¹ For a review, see B. Clerjaud, *J. Phys. C* **18**, 3615 (1985).

² A. V. Vasil'ev, G. K. Ippolitova, E. M. Omel'yanovskii, and A. M. Ryskin, *Sov. Phys. Semicond.* **10**, 341 (1976).

³ V. S. Vavilov and V. A. Morozova, *Sov. Phys. Semicond.* **20**, 226 (1986).

⁴ U. Kaufmann, H. Ennen, J. Schneider, R. Werner, J. Weber, and F. Kohl, *Phys. Rev. B* **25**, 5598 (1982).

⁵ P. S. Gladkov and K. B. Ozanyan, *J. Phys. C* **18**, L915 (1985).

- ⁶H. Terao, H. Sunakawa, K. Ohata, and H. Watanabe, in *Semi-Insulating III-V Materials*, *Evian*, 1982, edited by S. Makram-Ebeid and B. Tuck (Shiva, Nantwich, England, 1982), p. 54.
- ⁷M. Akiyama, Y. Karawada, and K. Kaminishi, *J. Cryst. Growth* **68**, 39 (1984).
- ⁸Y. Kawarada, M. Akiyama, and K. Kaminishi, in *Semi-Insulating III-V Materials*, *Hakone*, 1986, edited by H. Kukimoto and S. Miyazawa (North Holland/OHMSHA, Tokyo, 1986), p. 509.
- ⁹R. W. Hasty and G. R. Cronin, in *Physics of Semiconductors*, edited by M. Hulin (Dunod, Paris, 1964), p. 1161.
- ¹⁰W. Ulrich, K. Friedland, L. Eaves, and D. P. Halliday, *Phys. Status Solidi B* **131**, 719 (1985).
- ¹¹A. Mircea-Russel, G. M. Martin, and J. Lowther, *Solid State Commun.* **36**, 171 (1980).
- ¹²B. Clerjaud, C. Naud, B. Deveaud, B. Lambert, B. Plot-Chan, G. Bremond, C. Benjedou, G. Guillot, and A. Nouailhat, *J. Appl. Phys.* **58**, 4207 (1985).
- ¹³W. Kutt, D. Bimberg, M. Maier, H. Krautle, F. Kohl, and E. Bauser, *Appl. Phys. Lett.* **44**, 1078 (1984).
- ¹⁴W. Kutt, D. Bimberg, M. Maier, H. Krautle, F. Kohl, and E. Tomzig, *Appl. Phys. Lett.* **46**, 489 (1985).
- ¹⁵C. D. Brandt, A. M. Hennel, L. M. Pawlowicz, F. P. Dabkowski, J. Lagowski, and H. C. Gatos, *Appl. Phys. Lett.* **47**, 607 (1985).
- ¹⁶A. M. Hennel, C. D. Brandt, H. Hsiaw, L. M. Pawlowicz, F. P. Dabkowski, and J. Lagowski, *Gallium Arsenide and Related Compounds 1985*, Institute of Physics Conference Service No. 79 (Hilger, Bristol, 1986), pp. 43-48.
- ¹⁷A. M. Hennel, C. D. Brandt, L. M. Pawlowicz, and K. Y. Ko, in *Semi-Insulating III-V Materials*, *Hakone*, 1986, edited by H. Kukimoto and S. Miyazawa (North Holland/OHMSHA, Tokyo, 1986), p. 465.
- ¹⁸T. Bryskiewicz, in *Semiconductor Optoelectronics*, edited by M. A. Herman (PWN-Polish Scientific, Warsaw, 1980), pp. 187-212; in *Progress in Crystal Growth and Characterization*, edited by B. Pamplin (Pergamon, Oxford, in press).
- ¹⁹T. Bryskiewicz, C. F. Boucher, Jr., J. Lagowski, and H. C. Gatos, *J. Cryst. Growth* (to be published).
- ²⁰J. Lagowski, H. C. Gatos, C. H. Kang, M. Skowronski, K. Y. Ko, and D. G. Lin, *Appl. Phys. Lett.* **49**, 892 (1986).
- ²¹D. C. Look, in *Semiconductors and Semimetals*, edited by R. K. Willardson and A. C. Beer (Academic, New York, 1983), Vol. 19, p. 75.
- ²²W. Walukiewicz, J. Lagowski, L. Jastrzebski, M. Lichtensteiger, and H. C. Gatos, *J. Appl. Phys.* **50**, 899 (1979).
- ²³W. Walukiewicz, J. Lagowski, and H. C. Gatos, *J. Appl. Phys.* **53**, 76 (1982).
- ²⁴C. D. Brandt, A. M. Hennel, L. M. Pawlowicz, Y.-T. Wu, T. Bryskiewicz, J. Lagowski, and H. C. Gatos, *Appl. Phys. Lett.* **48**, 1162 (1986).
- ²⁵M. Caldas, S. K. Figueiredo, and A. Fazzio, *Phys. Rev. B* **33**, 7102 (1986).
- ²⁶P. W. Yu (private communication).
- ²⁷H. Katayama-Yoshida and A. Zunger, *Phys. Rev. B* **33**, 2961 (1986).
- ²⁸See, for example, K. Kocot and J. M. Baranowski, *Phys. Status Solidi B* **81**, 629 (1977); A. P. Radlinski, *Phys. Status Solidi B* **84**, 503 (1977).
- ²⁹B. Clerjaud (private communication).
- ³⁰C. D. Brandt (unpublished).
- ³¹L. A. Ledebo and B. K. Ridley, *J. Phys. C* **15**, L961 (1982).
- ³²M. J. Caldas, A. Fazzio, and A. Zunger, *Appl. Phys. Lett.* **45**, 671 (1984).
- ³³G. Bremond, A. Nouailhat, G. Guillot, B. Deveaud, B. Lambert, Y. Toudic, B. Clerjaud, and C. Naud, in *Microscopic Identification of Electronic Defects in Semiconductors*, Materials Research Society Symposia Proceedings, edited by N. M. Johnson, S. G. Bishop, and G. D. Watkins, (Materials Research Society, Pittsburgh, 1985), Vol. 46, p. 359.
- ³⁴B. Deveaud, B. Plot, B. Lambert, G. Bremond, G. Guillot, A. Nouailhat, B. Clerjaud, and C. Naud, *J. Appl. Phys.* **59**, 3126 (1986).
- ³⁵C. D. Brandt, A. M. Hennel, J. Lagowski, and H. C. Gatos (unpublished).
- ³⁶B. Lambert, B. Deveaud, Y. Touduc, G. Pelous, J. C. Paris, and G. Grandpierre, *Solid State Commun.* **47**, 337 (1983).
- ³⁷W. Ulrich, L. Eaves, K. Friedland, D. P. Halliday, and J. Kreibl, in *Proceedings of the 14th International Conference on Defects in Semiconductors*, Paris, 1986 (to be published).
- ³⁸V. W. Rampton, M. K. Saker, and W. Ulrich, *J. Phys. C* **19**, 1037 (1986).
- ³⁹A.-M. Vasson, A. Vasson, C. A. Bates, and A. F. Labadz, *J. Phys. C* **17**, L837 (1984).
- ⁴⁰E. Litty, P. Leyral, S. Loualiche, A. Nouailhat, G. Guillot, and M. Lanoo, *Physica B* **117/118**, 182 (1983).

A STUDY OF ENERGY LEVELS INTRODUCED BY 3d TRANSITION ELEMENTS IN III-V COMPOUND SEMICONDUCTORS

by

CHARLES DAVID BRANDT

Submitted to the Department of Materials Science and Engineering on May 1, 1987 in partial fulfillment of the requirements for the degree of Doctor of Philosophy.

ABSTRACT

The present work focuses on the electronic characteristics of the deep levels introduced by the 3d transition elements vanadium, titanium, and scandium in the III-V compounds, especially with respect to their application in the growth of new thermally stable, semi-insulating GaAs and InP.

These elements were investigated in doped GaAs and InP crystals grown from the melt by the liquid encapsulated Czochralski and Horizontal Bridgman techniques, and from solution by liquid phase electroepitaxy. Through the application of advanced characterization techniques such as deep level transient spectroscopy, Hall effect measurements, optical absorption, and photoluminescence, the basic electronic and optical characteristics of deep levels introduced by these transition elements into GaAs and InP were determined.

In GaAs, the substitutional V³⁺/V²⁺ single acceptor level (V⁻/⁰) was identified at 0.15 ± 0.01 eV below the bottom of the conduction band in all crystals. From optical absorption measurements on p-type material, we further conclude that the V⁴⁺/V³⁺ donor level (V⁰/⁺) must be located within the valence band. We did not observe any midgap levels resulting from vanadium-impurity (defect) complexes. Thus, the energy position of the V³⁺/V²⁺ acceptor level cannot account for the reported semi-insulating properties of V-doped GaAs. We propose instead that vanadium acts as a gettering agent for residual shallow donors during crystal growth, resulting in the growth of undoped semi-insulating GaAs compensated by the deep native defect donor EL2.

An analysis of V-doped InP led to the identification of the V⁴⁺/V³⁺ donor positioned at $E_V + 0.24$ eV. No evidence of the V³⁺/V²⁺ acceptor level was found, indicating that it is positioned above the bottom of the

conduction band. Vanadium is therefore not suitable for the growth of semi-insulating InP.

Titanium was found to introduce two deep levels in GaAs which were identified as the $\text{Ti}^{3+}/\text{Ti}^{2+}$ single acceptor level ($\text{Ti}^{-/0}$) at $E_c - 0.23$ eV and the $\text{Ti}^{4+}/\text{Ti}^{3+}$ donor level ($\text{Ti}^{0/+}$) at $E_c - 1.00$ eV. The position of these levels within the energy gap preclude their use for the growth of high resistivity GaAs. Upon consideration of the Vacuum Referred Binding Energies of these Ti levels in GaAs however, the potential midgap position of the $\text{Ti}^{4+}/\text{Ti}^{3+}$ donor in InP was discovered. Characterization of Ti-doped InP crystals resulted in the identification of the $\text{Ti}^{4+}/\text{Ti}^{3+}$ donor level near midgap at $E_c - 0.63$ eV, with the corresponding $\text{Ti}^{3+}/\text{Ti}^{2+}$ acceptor level lying within the conduction band. As a consequence of the midgap position of this donor level, we have developed a formulation for producing a new type of semi-insulating InP based on doping with Ti to compensate shallow acceptors. Resistivities in excess of $10^7 \Omega\text{-cm}$ can easily be obtained using this technique. This is the first semi-insulating III-V compound having a compensation mechanism based on a deep donor impurity. In view of the fact that Ti is expected to have a very low diffusivity in InP, it is of great technological significance that the thermal stability of Ti-doped semi-insulating InP should be superior to that of Fe-doped semi-insulating InP.

Measurements of both n and p-type GaAs crystals doped with Sc did not reveal the presence of any Sc-related deep levels. Deep level transient spectroscopy measurements extended to approximately 15K did not detect any Sc-related deep levels to within approximately 0.1 eV of either band edge. However, the optical absorption and photoluminescence features of n-type Sc-doped samples at 5K suggest the presence of a Sc-related deep level very close to the bottom of the conduction band. This level is proposed to be the $\text{Sc}^{3+}(3d^0)/\text{Sc}^{2+}(3d^1)$ single acceptor level ($\text{Sc}^{-/0}$) on the basis of both theoretical and experimental trends for the 3d transition element single acceptor levels in GaAs.

Thesis Supervisors:

Harry C. Gatos
Title: Professor of Electronic Materials

Jacek Lagowski
Title: Senior Research Associate

IMPURITY GETTERING BY TRANSITION ELEMENTS IN GaAs;
GROWTH OF SEMI-INSULATING GaAs CRYSTALS

by

KEI-YU KO

Submitted to the Department of Materials Science and
Engineering on January 8, 1988 in partial fulfillment of the
requirements for the degree of Doctor of Philosophy

Abstract

Semi-insulating GaAs, with resistivity in the range of 10^6 - 10^8 ohm-cm, is an important substrate material for high-speed integrated circuits and integrated optoelectronics. Problems with thermal stability and reproducible electrical parameters are limiting factors for widespread applications. In this work the electrical and optical characteristics of transition elements vanadium and titanium in GaAs were studied; their role as gettering agents through impurity interactions was discovered and investigated in detail to facilitate the use of vanadium and titanium for achieving a new type of thermally stable semi-insulating GaAs.

Through detailed study of crystals grown by Horizontal Bridgman and Liquid Encapsulated Czochralski techniques, we showed that the only energy level related to vanadium within the energy gap of GaAs was an acceptor level (V^{3+}/V^{2+}) at 0.15 ± 0.01 eV below the conduction band edge. No vanadium-related midgap level was observed by which vanadium could directly produce semi-insulating material. However vanadium was found to play a more subtle chemical role as a gettering agent for shallow donor impurities (Si and S) in the melt during solidification process, which led to the reduction in concentrations of shallow donor impurities (and thus electrically active species) in as grown crystals. Thermodynamic analysis of the gettering reactions in the melt was carried out regarding the concentrations of impurities in the melt and in the crystal. By controlled doping with vanadium and shallow acceptors in the Horizontal Bridgman case or by doping with vanadium alone in the Liquid Encapsulated Czochralski case, we have reproducibly grown thermally stable semi-insulating GaAs. It was shown that the compensation mechanism in these crystals was controlled by EL2 and that vanadium did not play a direct role in the

compensation process.

Titanium, on the other hand, was found to have no gettering effect with shallow donor impurities in GaAs. It simply incorporated as a substitutional impurity and gave rise to two deep levels within the GaAs energy gap. They are the Ti^{3+}/Ti^{2+} single acceptor level (-/o) at $E_c - 0.23$ eV and the Ti^{4+}/Ti^{3+} single donor level (o/+) at $E_v - 1.00$ eV. The positions of these energy levels indicates that titanium is not a practical dopant for producing semi-insulating GaAs crystal.

Thesis Supervisors:

Harry C, Gatos
Title: Professor of Electronic Materials

Jacek Lagowski
Title: Senior Research Associate

LPEE growth and characterization of $\text{In}_{1-x}\text{Ga}_x\text{As}$ bulk crystals

T. Bryskiewicz,* M. Bugajski,** B. Bryskiewicz, J. Lagowski and H.C. Gatos
Massachusetts Institute of Technology, Cambridge, MA 02139, USA

ABSTRACT: A novel procedure for liquid phase electroepitaxial (LPEE) growth of highly uniform multicomponent bulk crystals has been developed and successfully applied to the growth of high quality bulk $\text{In}_{1-x}\text{Ga}_x\text{As}$ crystals. $\text{In}_{1-x}\text{Ga}_x\text{As}$ ingots 14 mm in diameter and up to 3 mm thick were grown on (100)^z InP^x substrates. In terms of homogeneity, electrical characteristics, and defect structure they are comparable to high quality thin LPE layers.

1. INTRODUCTION

Liquid phase electroepitaxy is a solution growth technique in which the growth process is induced and sustained solely by passing a direct electric current across the solution-substrate interface while the temperature of the overall system is maintained constant (Bryskiewicz 1986 and references therein). It has been found that after initial stages of growth the solute electrotransport towards the interface becomes the dominant driving force for the growth (Bryskiewicz 1978, Jastrzebski et al 1978, Bryskiewicz et al 1980). Therefore, within a few minutes after an electric current is turned on the growth proceeds under isothermal and steady-state conditions. These features of electroepitaxy have proven (both experimentally and theoretically) to be uniquely suited for the growth of ternary and quaternary semiconductor compounds with constant composition (Daniele 1981, Bryskiewicz et al 1980). $\text{Ga}_{1-x}\text{Al}_x\text{As}$ wafers as thick as 600 μm (Daniele et al 1981), $\text{GaAs}_{1-x}\text{Sb}$ (Biryulin et al 1983), $\text{In}_{1-x}\text{Ga}_x\text{P}$ (Daniele et al 1983), and $\text{Hg}_{x}\text{Cd}_{1-x}\text{Tc}$ (Vanier et al 1980) epilayers up to 200 μm , 120 μm , and 500 μm , respectively, grown by LPEE showed a remarkable uniformity of composition, varying by $\Delta x=0.01-0.03$ over their entire thickness. However, the growth procedures proposed thus far (Daniele et al 1981, Nakajima 1987) are suitable for the growth of uniform wafers a few hundred microns thick.

In this paper a novel procedure, useful for electroepitaxial growth of bulk crystals (several millimeters thick) of ternary and quaternary semiconductors is proposed. This novel procedure is successfully applied to the growth of high quality $\text{In}_{1-x}\text{Ga}_x\text{As}$ bulk crystals.

2. NOVEL LPEE GROWTH PROCEDURE

The growth of highly uniform $\text{In}_{1-x}\text{Ga}_x\text{As}$ bulk crystals was carried out in a novel vertical LPEE apparatus (Bryskiewicz et al 1987a), employed recently

*On leave from Microgravity Research Associates, Inc., Midland, TX 79701, USA.

**On leave from Institute of Electron Technology, 02-668 Warsaw, Poland.

to the growth of epitaxial quality GaAs bulk crystals (Bryskiewicz et al 1987b). A schematic diagram of the growth cell used in our growth experiments is shown in Fig. 1. During electroepitaxial growth solution is

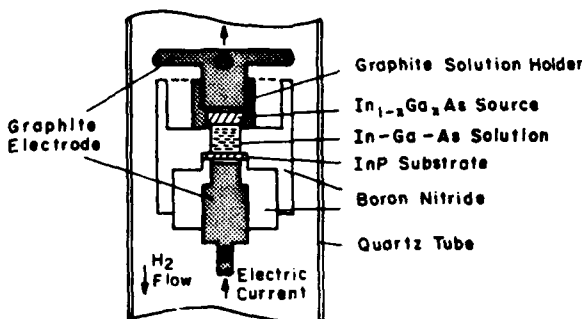


Fig. 1. Schematic diagram of the growth cell used for LPEE growth of $\text{In}_{1-x}\text{Ga}_x\text{As}$ bulk crystals.

contacted by the substrate at the bottom and the source material at the top. Thus, the crystallizing material driven by the electric current is deposited onto the substrate while the solution is being continuously saturated with the source material. A very important characteristic of the growth cell seen in Fig. 1 is the shape of a graphite source

holder which allows the current to bypass the source material. This results in a minimization of the Joule heating for an arbitrary form (monocrystal, polycrystal, or chunks) of the source material. The requirements for the source are thus limited to the compositional homogeneity and the chemical composition fitted to the composition of the crystal to be grown. In order to achieve these source characteristics, a procedure for the preparation of a macroscopically homogeneous source material had to be developed.

In this study the source material required for the growth of highly uniform $\text{In}_{1-x}\text{Ga}_x\text{As}$ bulk crystals was prepared in a sealed quartz ampoule evacuated to 10^{-6} Tr. The inner wall of the quartz ampoule was covered with a pyrolytic carbon in order to prevent wetting. A semiconductor grade InAs-GaAs quasibinary mixture and a small amount of a high purity arsenic were sealed in the ampoule, heated up to about 20-30°C above the liquidus temperature and kept molten for one hour. High compositional homogeneity of the $\text{In}_{1-x}\text{Ga}_x\text{As}$ source material was assured by rapid cooling of the ampoule. $\text{In}_{1-x}\text{Ga}_x\text{As}$ bulk crystals with compositions between $x=0.46$ and $x=0.48$ were grown at 650°C on (100)-oriented, Sn-doped InP substrates. The grown ingots were 14 mm in diameter and up to 3 mm thick, i.e., suitable for slicing up to five wafers.

3. CRYSTAL CHARACTERIZATION

A microphotograph of the etch pits revealed on the (100)-oriented InP substrate and on the $\text{In}_{0.52}\text{Ga}_{0.48}\text{As}$ bulk crystal is seen in Fig. 2. Although the dislocation loops generation process is very likely to occur in this case near the surface, we did not observe any significant increase in the etch pit density between the InP substrate ($\text{EPD} \sim 5-2 \times 10^5 \text{ cm}^{-2}$) and $\text{In}_{1-x}\text{Ga}_x\text{As}$ crystals.

Electrical parameters of the $\text{In}_{1-x}\text{Ga}_x\text{As}$ bulk crystals grown from unbaked In-rich solutions are shown in Table I. It is expected that the free electron concentration in the low 10^{16} cm^{-3} range can be reduced considerably by using higher purity solution components and/or by baking the solution prior to each run (Bhattacharya et al 1983). The 300°K mobility as high as $8000 \text{ cm}^2/\text{Vs}$ and the 77°K mobility of about $13,000 \text{ cm}^2/\text{Vs}$ is

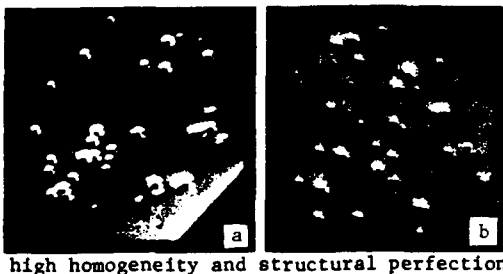


Fig. 2. Optical micrographs showing the typical etch pit pattern observed on (a) (100)-oriented InP substrate; (b) $\text{In}_{0.52}\text{Ga}_{0.48}\text{As}$ bulk crystal.

quite remarkable for the 10^{16} cm^{-3} free carrier concentration. These mobility values suggest low compensation and high homogeneity and structural perfection of the $\text{In}_{1-x}\text{Ga}_x\text{As}$ ingots.

Table I. Electrical characteristics of LPEE $\text{In}_{1-x}\text{Ga}_x\text{As}$ bulk crystals.

Composition (at.%)	Conductivity Type	Carrier Concentration (cm^{-3})		Mobility (cm^2/Vs)	
		300°K	77°K	300°K	77°K
46	n	2.7×10^{16}	2.4×10^{16}	6240	13620
47	n	4.5×10^{16}	4.1×10^{16}	7780	11750
48	n	4.6×10^{16}	4.0×10^{16}	7640	13140

In addition, DLTS measurements did not reveal any measurable electron traps in these crystals.

Structural perfection as well as high compositional homogeneity of the $\text{In}_{1-x}\text{Ga}_x\text{As}$ bulk crystals, comparable in quality with thin LPE layers, is documented by a high resolution photoluminescence (PL) spectrum shown in Fig. 3. This spectrum was recorded at 5°K for a nominally undoped n-type

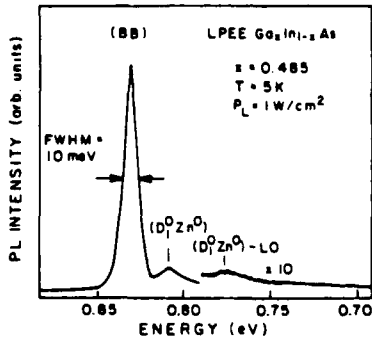


Fig. 3. 5°K PL spectrum of n-type $\text{In}_{0.52}\text{Ga}_{0.48}\text{As}$ grown on (100) InP substrate; $x = 0.485$, $T = 5\text{ K}$, $P_L = 1\text{ W}/\text{cm}^2$.

LPEE $\text{Ga}_{0.52}\text{Ga}_{0.48}\text{As}$ crystal. The dominant line at 0.8303 eV corresponds to the band-to-band transitions (BB). The above assignment was made on the basis of the line shape and the luminescence intensity vs. excitation density dependence (which appeared to be nearly quadratic). As seen in Fig. 3, the full width at half maximum (FWHM) of the (BB) line is equal to 10 meV. This value can be understood in terms of alloy broadening

due to the random distribution of the In and Ga cations. From the model developed for $\text{Al}_x\text{Ga}_{1-x}\text{As}$ (Schubert et al 1984) the alloy broadening of the BB transitions in $\text{In}_{1-x}\text{Ga}_x\text{As}$ has been estimated to be in the 9.2–13.7 meV range. The spread in the calculated FWHMs results mainly from the uncertainties of the values of the heavy hole mass and band discontinuity at the $\text{In}_{1-x}\text{Ga}_x\text{As}/\text{InP}$ heterointerface. Nevertheless, an overall agreement between theory and experiment is satisfactory.

The second line in Fig. 3 located 20.4 meV below the (BB) peak is due to the presence of the residual Zn acceptor, and it corresponds to the donor-

acceptor (DA) type of transitions. The binding energy E_A of the Zn acceptor estimated from the line position in different samples is $E_A = 20.6 - 21.5$ meV, in close agreement with $E_A = 22 \pm 1$ meV reported by Goetz et al (1983).

The measurements of the (BB) peak position were used to determine the compositional variations vs. a distance from the substrate and along the crystal surface. The results are shown in Fig. 4a and b, respectively. An excellent compositional homogeneity of the $\text{In}_{1-x}\text{Ga}_x\text{As}$ ingots, both perpendicular and parallel to the growth direction, is evident. In both cases the composition fluctuations do not exceed 1%.

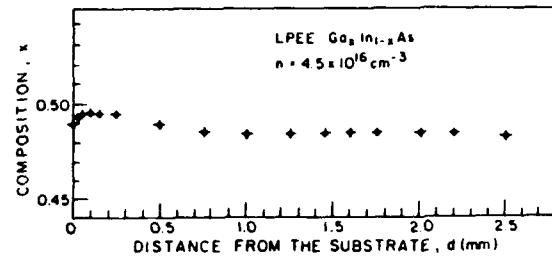
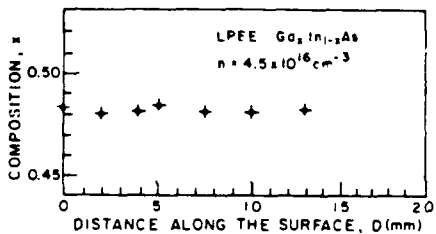


Fig. 4. Composition profile of $\text{In}_{0.52}\text{Ga}_{0.48}\text{As}$ obtained from PL measurements:
(a) along the growth direction



(b) perpendicular to the growth direction.

The authors are grateful to Microgravity Research Associates, Inc., and to the Air Force Office of Scientific Research for financial support.

4. REFERENCES

- Bhattacharya P K, Rad M V and Tsai M-J 1983 *J. Appl. Phys.* 54, 5096
 Biryulin Y F, Golubev L V, Novikov S V and Shmartsev Yu V 1983 *Sov. Tech. Phys.* 9, 68 (*Pis'ma Zh. Tekh. Fiz.* 9, 155)
 Bryskiewicz T 1978 *J. Cryst. Growth* 43, 567
 Bryskiewicz T, Lagowski J and Gatos H C 1980 *J. Appl. Phys.* 51, 988
 Bryskiewicz T 1986 *Prog. Crystal Growth and Charact.* 12, 29 (Pergamon)
 Bryskiewicz T, Boucher Jr C F, Lagowski J and Gatos H C 1987a *J. Cryst. Growth* 82, 279
 Bryskiewicz T, Bugajski M, Lagowski J and Gatos H C 1987b *J. Cryst. Growth* (to be published)
 Daniele J J and Hebling A J 1981 *J. Appl. Phys.* 52, 4325
 Daniele J J and Lewis A 1983 *J. Electron. Mat.* 12, 1015
 Goetz K H, Bimberg D, Jurgensen H, Selders J, Solomonov A V, Glinski G F and Razeghi M 1983 *J. Appl. Phys.* 54, 4543
 Jastrzebski L, Lagowski J, Gatos H C and Witt A F 1978 *J. Appl. Phys.* 49, 5909; 50, 7269 (1979)
 Nakajima K 1987 *J. Appl. Phys.* 61, 4626
 Schubert E F, Gobel E O, Horikoshi Y, Ploog K and Queisser H J 1984 *Phys. Rev. B* 30, 813
 Vanier P A, Pollak F H and Raccah P M 1980 *J. Electron. Mat.* 9, 153

Optical characterization of semi-insulating GaAs: Determination of the Fermi energy, the concentration of the midgap EL2 level and its occupancy

J. Lagowski, M. Bugajski,^{a)} M. Matsui,^{b)} and H. C. Gatos
Massachusetts Institute of Technology, Cambridge, Massachusetts 02139

(Received 6 April 1987; accepted for publication 17 June 1987)

The key electronic characteristics of semi-insulating GaAs, i.e., the Fermi energy, concentration, and occupancy of the midgap donor EL2, and the net concentration of ionized acceptors can all be determined from high-resolution measurements of the EL2 intracenter absorption. The procedure is based on the measurement of zero-phonon line intensity before and after the complete transfer of EL2 to its metastable state followed by thermal recovery. The procedure is quantitative, involves no fitting parameters, and unlike existing methods, is applicable even when a significant part of the EL2 is ionized.

Electronic parameters of semi-insulating (SI) GaAs and its behavior during device processing depend on the concentration of the native deep donor EL2 and the net concentration of ionized acceptors.¹ Currently, the evaluation of such pertinent parameters is carried out employing a combination of optical and electrical measurements.¹⁻⁴ The concentration of EL2 is evaluated from the near-infrared optical absorption, while Hall effect and electrical conductivity measurements yield the Fermi energy from which the EL2 occupancy can be calculated. The concentration of ionized EL2 provides, of course, a measure of the net ionized acceptor concentration. The knowledge of the Fermi energy is crucial, since optical absorption measurements alone cannot differentiate between changes in EL2 occupancy and EL2 concentration. Thus, the reliability of the optical absorption procedure for the determination of the EL2 concentration, as commonly employed, is decreased as the fraction of the ionized EL2 becomes significant, i.e., in *n*-type SI GaAs with resistivities exceeding $10^8 \Omega \text{ cm}$ and in *p*-type SI GaAs.

In this letter we discuss a characterization approach which is based on measurements of optical absorption, but it is applicable to both *n*- and *p*-type SI GaAs.

The difference between the present approach and earlier approaches is twofold. Firstly, we utilize the EL2 intracenter absorption rather than the total EL2 absorption band. The intracenter absorption is uniquely related to the neutral (occupied) state of EL2 in contrast to the total absorption, in which the photoionization transitions from the occupied EL2 state to the conduction band are involved as well as those from the valence band to the ionized EL2 state.^{4,5} Secondly, we utilize the optical excitation of EL2 to its metastable state⁶ in order to transfer the entire concentration of EL2 into the neutral state. In the standard approaches the metastable state is used to determine the background absorption which is not related to EL2.³

The proposed procedure involves three steps: (1) the SI GaAs sample is cooled in the dark from room temperature to 6 K; (2) EL2 is optically bleached (with white light); and

(3) the sample is annealed at 120–140 K and cooled back to 6 K. The optical absorption spectrum is measured after each step and the corresponding intensities of the zero-phonon line (α_{ZPL}^1 , α_{ZPL}^2 , and α_{ZPL}^3 , respectively) are used for the quantitative analysis. It is essential that the energy range from 1.037 and 1.041 eV, corresponding to the zero-phonon line,^{4,5} is recorded with enhanced resolution and sensitivity.

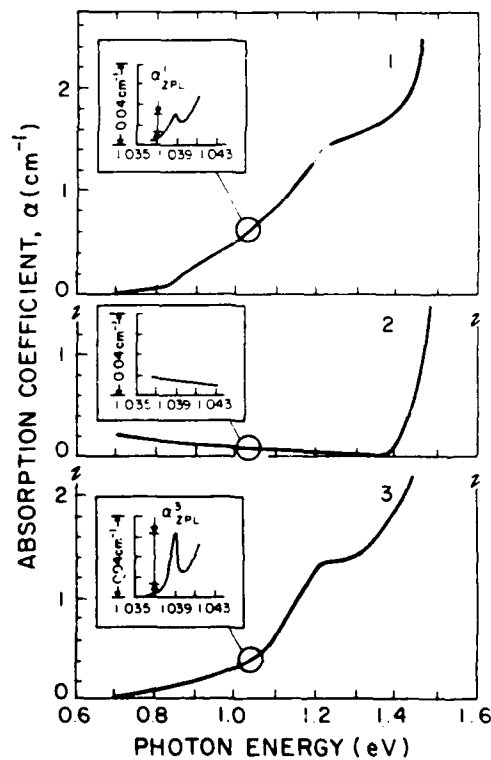


FIG. 1. 6 K optical absorption spectra of GaAs with the EL2 occupancy fraction $f=0.3$ at 300 K: 1—after cooling from 300 K, 2—after absorption bleaching; and 3—after subsequent annealing at 140 K for 5 min. Insets show the zero-phonon line absorption.

^{a)}On leave from Institute of Electron Technology, Warsaw, Poland.

^{b)}On leave from Sumitomo Metal Mining Co., Ltd., Tokyo, Japan.

Furthermore, the measurements must be carried out with very low intensity incident light in order to prevent any measurable transfer of EL2 into its metastable state during the measurements following steps (1) and (2).

In order to demonstrate the new procedure we take an example of undoped SI GaAs with a relatively low value of Hall effect mobility at 300 K (about $3000 \text{ cm}^2/\text{V s}$) and very high resistivity (about $5 \times 10^8 \Omega \text{ cm}$). In such material a significant fraction of EL2 is expected to be ionized² and thus the standard optical method based on Ref. 3 is not readily applicable. The optical spectra taken after steps (1), (2), and (3), and denoted as (1), (2), and (3), respectively, are shown in Fig. 1. Spectrum (1) reflects the ionized state of EL2 frozen from room temperature. This spectrum is different from the EL2 absorption band characteristic of *n*-type conducting GaAs where EL2 is completely neutral. On the other hand, the zero-phonon line (see insert) is clearly observed and provides a measure of the concentration of neutral EL2. Illumination with strong white light [step (2)] eliminates the entire spectrum, including the zero-phonon line (see spectrum 2). EL2 is entirely in its metastable state which is neutral, and optically inactive. Annealing at 140 K for 5 min transforms EL2 back to its normal, optically active, state, without changing its occupancy. As a result, spectrum (3) corresponds to EL2, which is entirely neutral. As can be seen, about a threefold increase in the zero-phonon line intensity is observed in comparison to spectrum (1). The whole absorption band also changes its shape becoming similar to the characteristic absorption of conducting *n*-type GaAs.

The zero-phonon line intensity ratio $\alpha_{ZPL}^1 / \alpha_{ZPL}^3 = f_n$ provides a direct measure of the EL2 occupancy factor $f_n = n_{EL2}^0 / N_{EL2}$ (where n_{EL2}^0 and N_{EL2} represent neutral and total EL2 concentration, respectively). The Fermi energy with respect to the bottom of the conduction band becomes $E_c - E_F = kT \ln(f_n^{-1} - 1) + E_{EL2}^1$, where E_{EL2}^1

$= 0.759 - 0.237 \times 10^{-3} T$ ^{2.8} is "effective" EL2 energy which includes a contribution from the degeneracy factor. It must be emphasized that the occupancy factor f_n or the Fermi energy E_F can be used to determine the conductivity type and the free electron and hole concentrations.^{1,4} If prior to cooling [step (1)], the sample is equilibrated in the dark at 300 K, the f_n and E_F values can be taken as representative of this temperature. From existing calculations in Refs. 2 and 9, f_n and E_F at 300 K can be related to values of resistivity (or conductivity), free-carrier concentration, and Hall effect mobility.

A recent high-resolution optical and transient capacitance study⁴ of EL2 provided a quantitative relation between α_{ZPL} and n_{EL2}^0 , i.e., $\alpha_{ZPL} / n_{EL2}^0 = 1.1 \times 10^{-18} \text{ cm}^2$. This ratio is insensitive to temperature between 2 to 10 K. The total EL2 concentration estimated from α_{ZPL}^1 becomes $N_{EL2} = 0.9 \times 10^{18} \text{ cm}^3$. The concentration of ionized EL2 is given by $n_{EL2}^+ = 0.9 \times 10^{18} (\alpha_{ZPL}^1 - \alpha_{ZPL}^3)$. Considering electrical neutrality, the net concentration of ionized acceptors we have is $N_A^- - N_D^+ = n_{EL2}^+$ (where N_D^+ refers to ionized donors other than EL2).

For example, the set of electrical parameters evaluated from optical measurements for the crystal analyzed in Fig. 1 is as follows: $N_{EL2} = 1.5 \times 10^{16} \text{ cm}^{-3}$, $n_{EL2}^0 = 5 \times 10^{15} \text{ cm}^{-3}$, $N_A^- - N_D^+ = 1.0 \times 10^{16} \text{ cm}^{-3}$, $f_n = 0.3$, $E_c - E_F = 0.73 \text{ eV}$, $\rho(300 \text{ K}) \approx 7 \times 10^8 \Omega \text{ cm}$, $\mu_H \approx 3500 \text{ cm}^2/\text{V s}$, $p(300 \text{ K}) \approx 5 \times 10^6 \text{ cm}^{-3}$. We should point out that conductivity and Hall effect measurements yielded resistivity and Hall effect mobility values within 20% from above estimates.

Application of the present approach to different SI GaAs with high Hall effect mobility ($\mu_H > 5000 \text{ cm}^2/\text{V s}$) and relatively low resistivity (300 K resistivity below $10^8 \Omega \text{ cm}$) is illustrated in Fig. 2. In such material the majority of EL2 is expected to be neutral. Indeed, only a very small enhancement of the zero-phonon line intensity was observed after step (3). Actually, the ratio $f_n = \alpha_{ZPL}^1 / \alpha_{ZPL}^3 = 0.98$ implies that only 2% of EL2 is ionized. Quantitative analysis yields the following values of the other parameters $E_c - E_F = 0.64 \text{ eV}$, $N_{EL2} = 3.6 \times 10^{16} \text{ cm}^{-3}$, $n_{EL2}^0 = N_A^- - N_D^+ = 1.6 \times 10^{15} \text{ cm}^{-3}$. In this case the standard

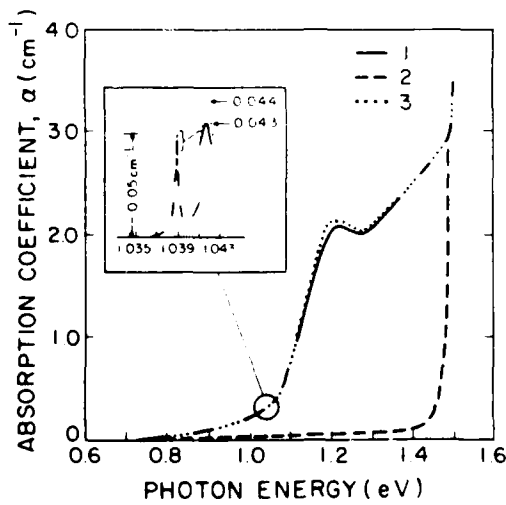


FIG. 2. 6 K optical absorption spectra of standard SI GaAs with majority of EL2 occupied at 300 K. 1, 2, and 3 correspond to the same conditions as in Fig. 1.

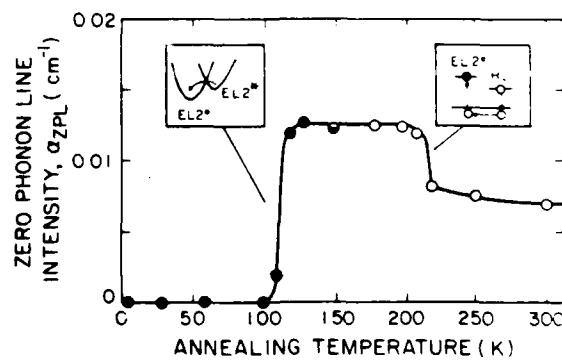


FIG. 3. Zero-phonon line intensity vs the annealing temperature of step (3), used to recover the EL2 from the metastable state. Filled and open circles correspond to annealing time of 10 and 15 min, respectively.

method for the determination of EL2 concentration from the total optical absorption at $\lambda = 1.06 \mu\text{m}$ can be conveniently employed. Indeed, this standard method yielded $N_{\text{EL2}} = 3.4 \times 10^{16} \text{ cm}^{-3}$ (using the revised calibration factor after Ref. 4) in very good agreement with the present approach.

It should be pointed out that EL2 is the dominant midgap level in GaAs crystals grown by the standard methods from As-rich melts.⁷ Other midgap levels are present, but at concentrations about one magnitude smaller than that of EL2. Since the zero-phonon line employed here is uniquely related to EL2 with a specific signature,⁵ our approach for the determination of the EL2 concentration remains valid, even in the presence of other midgap levels at concentrations comparable to those of EL2. In such a case, however, the concentration of ionized EL2 cannot be taken as an exact measure of concentration of the net ionized acceptors but rather as the lower limit of $N_A - N_D$.

In the course of this investigation we found that the intensity of the zero-phonon line, α_{ZPL}^3 , reaches a constant value for annealing temperatures $T_A > 120 \text{ K}$, consistent with the established EL2 behavior in SI GaAs. Beyond 220 K, however, α_{ZPL}^3 decreases significantly, as shown in Fig. 3. Measurements of thermally stimulated current (TSC) showed that this decrease is associated with the thermal emission of holes (trapped during illumination at low temperatures by hole traps HL3, HL9, and HL10)¹⁰ and their recombination with EL2 electrons. Thus, if relatively shallow hole traps are present at high densities, a decrease of α_{ZPL}^3 can in general take place. This potentially interfering process can be recognized (using additional TSC measurements) and minimized by adjusting the annealing conditions, i.e., temperature and annealing time.

In summary, we have shown that high-resolution measurements of the 1.039 eV zero-phonon line can be very effectively applied for the optical characterization of SI GaAs. This approach has fundamental advantages over the standard optical method for the determination of the EL2 concentration in the characterization of materials in which EL2 is partially ionized. It should prove particularly useful in the characterization of a new type of GaAs crystal exhibiting inverted thermal conversion (ITC) in which very high resistivity is achieved by thermal annealing.¹¹ The standard optical method is not suitable for ITC GaAs because in this material a significant fraction of EL2 is ionized.

The authors are grateful to the National Aeronautics and Space Administration and to the Air Force Office of Scientific Research for financial support.

- ¹G. M. Martin, J. P. Farges, G. Jacob, and J. P. Hallais, *J. Appl. Phys.* **51**, 2840 (1980).
- ²W. Walukiewicz, J. Lagowski, and H. C. Gatos, *Appl. Phys. Lett.* **43**, 192 (1983).
- ³G. M. Martin, *Appl. Phys. Lett.* **39**, 747 (1981).
- ⁴M. Skowronski, J. Lagowski, and H. C. Gatos, *J. Appl. Phys.* **59**, 2451 (1986).
- ⁵M. Kaminska, M. Skowronski, and W. Kuszko, *Phys. Rev. Lett.* **55**, 2204 (1985).
- ⁶G. Vincent, D. Bous, and A. Chantre, *J. Appl. Phys.* **53**, 3643 (1982).
- ⁷H. C. Gatos and J. Lagowski, *Mater. Res. Soc. Symp. Proc.* **46**, 153 (1985).
- ⁸The revised value of the EL2 electron emission activation energy is used after Ref. 7. This value is slightly lower (by 10 meV) than the value used in Ref. 1.
- ⁹J. S. Blakemore, *J. Appl. Phys.* **53**, R123 (1982).
- ¹⁰G. M. Martin, in *Semi-Insulating III-V Materials*, edited by G. J. Rees (Shiva, Orpington, U.K., 1980), p. 13.
- ¹¹J. Lagowski, H. C. Gatos, C. H. Kang, M. Skowronski, K. Y. Ko, and D. G. Lin, *Appl. Phys. Lett.* **49**, 892 (1986).

Presented at 14th International Seminar on GaAs and Related Compounds,
Crete, Greece, October 1987.

Quantitative Correlation between the EL2 Midgap Donor, the 1.039 eV Zero Phonon Line, and the EPR Arsenic Antisite Signal

J. Lagowski, M. Matsui, M. Bugajski, C.H. Kang, M. Skowronski and H.C. Gatos and M. Hoinkis,* E.R. Weber,* and W. Walukiewicz*

Massachusetts Institute of Technology, Cambridge, MA 02139, USA

*Center for Advanced Materials, Lawrence Berkeley Laboratory,
University of California, Berkeley, CA 94720, USA

ABSTRACT: We provide the first quantitative evidence that in GaAs the EL2 midgap donor, the 1.039 eV zero phonon absorption line, and the EPR quadruplet are manifestations of one and the same defect. The EL2 donor corresponds to the (o⁺) state while the zero phonon line and the EPR quadruplet correspond to the neutral (o) and singly ionized (+) defect, respectively. The defect also exhibits the (+++) state 0.54 eV above the valence band and no other states in the energy gap.

1. INTRODUCTION

The native midgap donor EL2 in GaAs has been the subject of intensive studies motivated by a fundamental interest in the identity of this metastable defect and by the practical need for stringent control of EL2 during fabrication of integrated circuits. In a continuing search for the atomic structure of the EL2 defect three characteristic features have been the center of attention: energy levels of the defect, (Gatos and Lagowski 1985), the 1.039 eV zero phonon optical absorption line (ZPL) (Kaminska et al 1985), and the electron paramagnetic resonance (EPR) quadruplet signal (Weber et al 1982). All these features play an important role in linking the EL2 and the arsenic antisite defect As_{Ga}. A defect symmetry deduced from the behavior of ZPL in the uniaxial stress implies an isolated antisite As_{Ga}. The interpretation of EPR and ODENDOR is experiencing a continuous evolution of models from an isolated antisite through a distorted antisite to antisite aggregates and to As_{Ga}-As_I (Meyer et al 1986, von Bardeleben et al 1986). Recent theoretical calculations (Baraff and Schluter 1987) indicate that the As_{Ga}-As_I pair may be in conflict with the energy level structure of the EL2 defect. The above discrepancies created uncertainty and confusion which require careful re-examination of EL2-related properties.

2. EXPERIMENTAL APPROACH

Determination of quantitative relationships among the EL2, ZPL, and EPR quadruplet have been thus far impeded by (1) material incompatibility between EPR and DLTS techniques (which require high and low resistivity samples, respectively); (2) difficulties in controlling and measuring the Fermi energy in SI GaAs; (3) ambiguities associated with the "EL2 family", i.e., midgap levels other than EL2; and (4) very low intensity of the EPR quadruplet in SI GaAs. In the present study special attention was devoted to overcoming the above difficulties. Thus, the material incompatibility was resolved using conducting and high resistivity crystals subjected to identical thermal treatment. Optical characterization (applicable to both crystals) was then employed to verify EL2 behavior in SI GaAs. With the most recent version of the optical method (Lagowski et al 1987) we achieved

the determination of the total EL2 concentration as well as the EL2 occupancy and the Fermi energy. The inverted thermal conversion (ITC) treatment (Lagowski et al 1986) (i.e., 1200°C annealing-rapid quenching followed by 800-850°C annealing) was used to produce GaAs containing only EL2 and no other midgap levels. The DLTS spectrum of electron traps in such material shown in Fig. 1 indeed reveals only one high temperature peak. The corresponding capacitance transient is exponential (with the emission rate equal to the signature of EL2) (Gatos, Lagowski 1985).

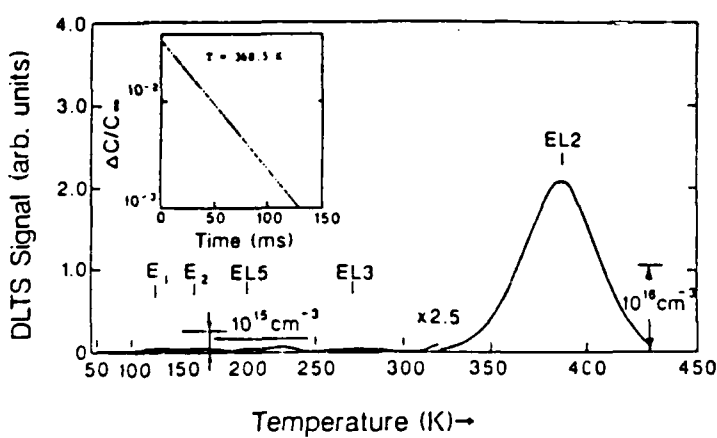


Fig. 1. DLTS spectrum of electron traps in GaAs after ITC+800°C, 1 h treatment, $t_1/t_2 = 5\text{ms}/10\text{ms}$.

In ITC GaAs EL2 concentration, N_{EL2} is typically 10^{15}cm^{-3} . 800-850°C annealing increases N_{EL2} to as much as $3 \times 10^{16}\text{cm}^{-3}$ depending on the annealing time and temperature. For undoped GaAs we used

this treatment in order to achieve predetermined concentration and occupancy of EL2. As shown in Fig. 2, a very strong EPR quadruplet signal is obtained in SI LEC GaAs after ITC+800°C treatment. The hyperfine splitting constant of the quadruplet is the same as the value originally reported by Wagner et al 1980 for the As^+ signal in as-grown GaAs. The strong quadruplet and readily resolvable ZPL illustrates advantages of our approach for the quantitative correlation of the EPR signal and ZPL.

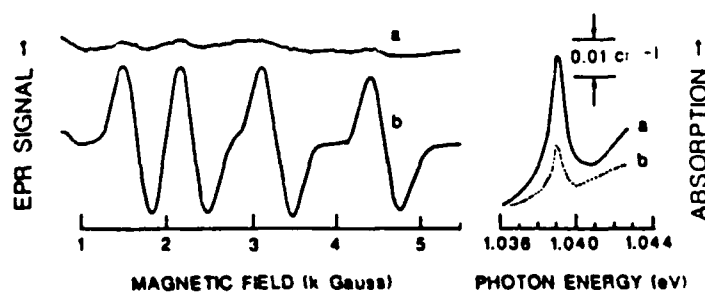


Fig. 2. EPR and ZPL in as-grown GaAs (a), and after ITC+800°C, 1 h treatment (b).

EPR measurements (4-300 K) were carried out using an X-band spectrometer interfaced to a computer. The apparatus had provisions for illumination of the sample in the cavity with either a monochromatic or white light. The absolute spin density corresponding to doubly integrated

EPR quadruplet was determined using P-doped silicon samples as standard and applying a very careful calibration procedure. The differences in microwave power characteristics and in temperature dependence of the EPR quadruplet (maximum of EPR absorption signal of the quadruplet occurred near 10 K) in GaAs and P-signal in silicon were taken into account. The results of EPR and optical absorption discussed below correspond to measurements done at 10 K.

The exact sequence of high resolution optical absorption and EPR measurements on undoped LEC GaAs subjected to ITC+800°C, 1 h, treatment is listed in Table I. The EPR measurements were made at Berkeley, while the optical absorption measurements on the sample were made at MIT. Special attention was placed on making the experimental conditions of the two experiments as similar as possible. The results given in Table I constitute a fragment of a larger experimental program involving measurements on a series of 24 samples: eight representing the as-grown material, eight after ITC treatment, and eight after ITC+800°C annealing. The values of N_{EL2}^0 (i.e., the concentration of occupied EL2) corresponding to a given zero phonon line absorption α_{ZPL} , were calculated using calibration provided by Skowronski et al 1986 for GaAs containing only one midgap level EL2. Estimated uncertainties are about $2 \times 10^{15} \text{ cm}^{-3}$ for N_{EL2}^0 and about 20% for the spin density.

Table I. Sequence of measurements employed for correlation of EPR quadruplet (QT) and ZPL

EXPERIMENTAL STEPS	ZPL (10^{-2} cm^{-1})	N_{EL2}^0 (10^{16} cm^{-3})	QT (arb. units)	EPR	N_s (10^{16} cm^{-3})	$N_{EL2+N_s}^0$ (10^{16} cm^{-3})
1. Cooling from 300 K in dark	0.75	0.6	27	1.8	2.4	
2. White light illumination ^(a)	0	0	0	0	--	
3. 150 K; 10 min ^(b)	1.9	1.7	11	0.7	2.4	
4. Illumination; 0.9 μm , 30 min ^(c)	1.3	1.2	20	1.3	2.5	
5. 150 K, 10 min ^(b)	1.1	1.0	23	1.5	2.5	
6. White light illumination ^(a)	0	0	0	0	--	
7. 150 K, 10 min ^(b)	2.6	2.3	4.6	0.3	2.6	
8. Illumination, 2.5 μm , 30 min ^(c)	2.4	2.2	6	0.4	2.6	
9. Illumination, 1.3 μm , 30 min ^(c)	2.5	2.25	0.2	0.1	2.4	

(a) Transfer to metastable state; (b) Recovery of normal state; (c) Photoionization.

3. RESULTS AND DISCUSSION

Quantitative results given in Table I were also used to construct a plot of the intensity of the EPR QT signal vs. the intensity of the zero phonon line. This plot shown in Fig. 3 demonstrates the one-to-one correlation between a decrease in spin density and increase in the concentration of the neutral EL2. The data in Table I prove that this correlation remains valid during the photoionization of EL2 (0.9 μm illumination) or photo-population of EL2 by photoexcitation of holes to the valence band (1.3 μm illumination) as well as upon recovery of EL2 from the metastable state. It is also seen that the transfer of EL2 to a metastable state (by white light illumination) eliminates both the ZPL and the EPR quadruplet. With the exception of this specific case (steps 2 and 6) the concentration of the neutral EL2 plus the spin density remains constant $N_{EL2+N_s}^0 = (2.5 \pm 0.1) \times 10^{16} \text{ cm}^{-3}$. This value coincides with the total EL2 concentration, N_{EL2}^0 . We thus conclude that the changes in α_{ZPL} and QT signal shown in Fig. 3 are brought about by the changes in the occupation of EL2. We further conclude that the midgap EL2 donor, the ZPL and EPR quadruplet are the manifestations of different charge states of one and the same defect. The EL2 donor corresponds to the (0/+) state of the defect. The zero phonon line and the EPR quadruplet correspond to the neutral (0) and singly ionized (+) defect, respectively. An additional (+++) level of the defect is located 0.54 eV above the valence band. This level acts as a hole trap and is visible in photo EPR (Weber et al 1982), DLTS, and photo-DLTS (Gatos and Lagowski 1985). No other EL2 level exists in the upper half of the

energy gap. Such level, if present, would have to be seen in the DLTS spectrum of Fig. 1.

The results of the present study should be viewed as a quantitative empirical unification of EL2 properties. This unification, however, leads to the interpretational dilemmas and the following sequence of conflicts:

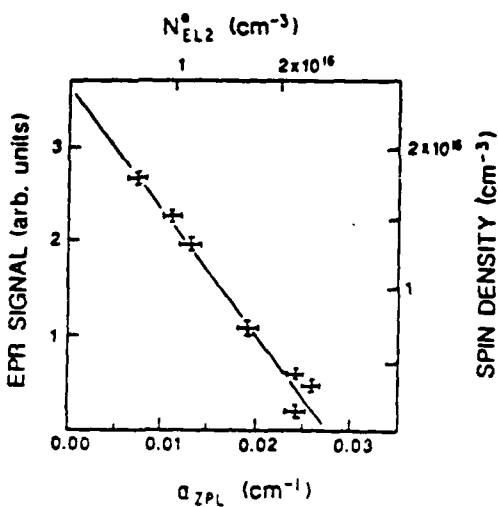


Fig. 3. See text.

The MIT contribution was sponsored by NASA and the USAFOSR. The contribution from Berkeley was supported by the US Dept. of Energy under contract No. DE-AC03-76SF00098.

REFERENCES

1. G.A. Baraff and M. Schluter, Phys. Rev. B35, 6154 (1987).
2. H.J. von Bardeleben, D. Stievenard, D. Deremes, A. Huber and J.C. Bourgoin, Phys. Rev. B34, 7192 (1986).
3. H.C. Gatos and J. Lagowski, Mat. Res. Soc. Symp. Proc. 46, 153 (1985).
4. M. Kaminska, M. Skowronski, and W. Kuszko, Phys. Rev. Lett. 55, 2204 (1985).
5. J. Lagowski, M. Bugajski, M. Matsui, and H.C. Gatos, Appl. Phys. Lett. 51, 511 (1987).
6. J. Lagowski, H.C. Gatos, C.H. Kang, M. Skowronski, K.Y. Ko, and D.G. Lin, Appl. Phys. Lett. 49 892 (1986).
7. B.K. Meyer, D.M. Hofmann, and J.-M. Spaeth, Materials Science Forum, vol. 10, 311 (1986).
8. M. Skowronski, J. Lagowski, and H.C. Gatos, J. Appl. Phys. 59, 2451 (1986).
9. R.J. Wagner, J.J. Krebs, G.M. Stauss, and A.M. White, Solid State Commun. 36, 15 (1980).
10. E.R. Weber, H. Ennen, U. Kaufmann, J. Windscheif, J. Scheider, and T. Wosinski, J. Appl. Phys. 53, 6140 (1982).

ZPL interpretation that the isolated As₂ is the EL2 defect (Kaminska et al 1985) is in conflict with the pair As₂-As₂ posulated from ODENDOR (Meyer et al 1986) and EPR (von Bardeleben et al 1986). The theory (Baraff and Schluter 1987) states, however, that the pair cannot be the EL2 defect unless additional EL2 levels (other than (0/+) and the (+/++) at E = -0.75 eV and E = +0.54, respectively) exist in the upper half of the energy gap; experiments show that such levels do not exist. The above sequence must contain elements which are false. Their disclosure and the search for alternative interpretations of ZPL or ODENDOR are critical for resolving the EL2 dilemma.

Effect of plastic deformation on electronic properties of GaAs

M. Skowronski,^{a)} J. Lagowski, M. Milstein,^{b)} C. H. Kang, F. P. Dabkowski,^{c)}

A. Hennel,^{d)} and H. C. Gatos

Massachusetts Institute of Technology, Cambridge, Massachusetts 02139

(Received 8 May 1987; accepted for publication 26 June 1987)

A systematic study of plastically deformed (in compression) GaAs was carried out employing deep-level spectroscopies, optical absorption, and electronic transport measurements. Deformation-induced changes in the free-carrier concentration, the mobility, and occupation of deep levels were associated with a deep acceptor defect. Changes of the optical absorption in deformed samples were found to be due to a localized stress field of dislocations rather than transitions via localized levels. No evidence was found of any meaningful increase ($> 2 \times 10^{15} \text{ cm}^{-3}$) of the concentration of EL2 or other midgap donors for deformation up to about 3%. Thus, it is evident that the enhancement of the electron paramagnetic resonance signal of the arsenic antisite As_{Ga} in deformed semi-insulating GaAs must be due to the increased ionization of As_{Ga} rather than the generation of new antisite defects.

I. INTRODUCTION

The relatively low mechanical strength of GaAs (the critical resolved shear stress about one order of magnitude smaller than that of silicon) causes melt-grown crystals to be very susceptible to plastic deformation induced by thermal gradients.^{1,2} The magnitude of thermal stresses can be particularly large in crystals grown by liquid encapsulated Czochralski (LEC). The dislocation density,¹⁻³ the electrical resistivity,⁴ and the optical transmissivity^{5,6} in such crystals exhibit spatial variations which often resemble the characteristic pattern of thermal stress. Similar patterns were also found in the leakage current^{7,8} and the threshold voltage variations of the enhancement mode field-effect transistors⁹ produced on semi-insulating (SI) LEC wafers. The understanding of these practically and fundamentally important results is at present very limited. In most instances it is not clear whether they reflect real cause to effect relations or coincidental processes only.

A number of investigations carried out in recent years was devoted to the effects of plastic deformation on electronic properties of GaAs.¹⁰⁻²² Deformation-induced deep and especially the main native deep donor EL2 and

related antisite defect As_{Ga} , were focal points in these studies.¹⁰⁻¹⁵ Early results obtained with deep-level transient spectroscopy (DLTS) seemed to indicate an increase of EL2 concentration during plastic deformation.¹³ Electron paramagnetic resonance (EPR) measurements on deformed SI GaAs crystals also showed an enhancement of the characteristic quadruplet line assigned to the singly ionized state of the arsenic antisite As_{Ga} .^{11,12,17} The similarity between the photoquenching of the EPR signal and the EL2-related photocapacitance spectra was taken as evidence of the common deformation related origin of the arsenic antisite and EL2.¹² More recent results of DLTS^{18,19} and of the optical absorp-

tion²⁰ imply that the EL2 concentration increases only very little (if at all) after plastic deformation. This finding contrasted with the behavior of the EPR signal and led to a hypothesis of different antisite complexes, all of which contribute to the EPR quadruplet, but only some to EL2.²¹ However, it has been pointed out that the enhancement of the EPR signal may be caused by deformation-induced acceptors which increase the concentration of ionized antisite As_{Ga} .²²

The present study addresses the question of deformation-induced midgap donors, the acceptors, and their effects on deep donor occupation. Optical and electronic properties of plastically deformed GaAs were investigated employing a series of *n*-type, SI, and *p*-type crystals, which enables the separation between the creation of new deep levels and the changes in population of the levels already present prior to deformation. Our experimental approach combined the measurements of DLTS (or thermally stimulated current for SI samples), Hall effect, and optical absorption performed on the same samples. In addition, deformed samples were subsequently subjected to thermal annealing in order to evaluate the stability of deformation-induced defects.

II. EXPERIMENT

A. Sample preparation

Conducting *n*- and *p*-type crystals used in this study were grown from the melt in this laboratory. For *n*-type samples selenium was used as a dopant, and the resulting net carrier concentration was $5-10 \times 10^{16} \text{ cm}^{-3}$. The mobility was in excess of $3000 \text{ cm}^2/\text{V s}$. *p*-type crystals were doped with zinc. Two sets of samples were used with 300-K hole concentration of 5×10^{15} and $5 \times 10^{16} \text{ cm}^{-3}$, respectively. The dopant concentration in all cases was low enough to prevent the effects of impurity hardening and to avoid changes in the mechanical properties of the crystals. Prior to deformation, whole ingots were annealed for 12 h at 850°C under As overpressure to assure thermal stability of the starting material and to relieve any residual built-in stress. The ingots were subsequently cut in the form of rectangular slabs $4 \times 4 \times 7 \text{ mm}^3$ with the long axis (111), (110), or

^{a)} Present address: Cabot Corporation, Billerica, MA 01821.

^{b)} Present address: 781 Hamilton St., Somerset, NJ 08873.

^{c)} Present address: Polaroid Corporation, Cambridge, MA 02139.

^{d)} Present address: Institute of Experimental Physics, Warsaw University, Warsaw, Poland.

(100) being in the direction of applied stress. Each sample used in the experiment had its own reference sample cut in the immediate vicinity from the same crystal. The reference samples have undergone the same thermal treatment as the deformed specimens to precisely determine the effects of deformation.

The samples for capacitance measurements were lapped and chemically polished, and immediately afterward were placed in the evaporator. For *n*- and *p*-type GaAs the metal-semiconductor Schottky diodes were formed by evaporation of gold and aluminum, respectively. All diodes were carefully tested for the leakage current density and the breakdown voltage.

B. Plastic deformation

Deformation, in a compression mode, was performed at 400 °C in an "Instron" tensile machine equipped with a load cell. The sample with the length l_0 of 7 mm, was placed between two alumina cylinders located inside the resistance furnace which controlled the sample temperature within 5 °C. Deformation was realized by compressing the sample at a constant rate dl/dt of 0.05 mm/min. The load cell was used to monitor the applied force. All samples used in this study showed a gradual increase in the compression stress and a monotonic decrease of the length. The samples with irregular response to deformation were rejected from further study since they might have contained internal cracks. The degree of deformation $\Delta l/l_0$ was determined by careful measurements of sample length l_0 before and l_1 after deformation. For easy comparison a deformation was realized in all three directions, (100), (110), and (111), employed in previous studies.¹⁰⁻²² The degree of deformation $\Delta l/l_0$ was varied between 0% and 4%.

C. Characterization

Plastically deformed and reference samples were subjected to identical electrical and optical characterization. Thus, the electrical conductivity and Hall-effect measurements were performed using van der Pauw configuration. Optical absorption measurements were done with a near-infrared high-resolution spectrometer. The sample was placed on a cold finger in a variable temperature liquid-He cryostat. Absorption spectra were measured using very low-intensity incident light in order to prevent EL2 transfer into the metastable state. Deep-level characterization was carried out with standard deep-level transient capacitance measurements using a box-car averager. Optical deep-level transient capacitance spectroscopy was also employed for the hole trap determination in *n*-type GaAs. Deep levels in semi-insulating GaAs were analyzed by the thermally stimulated current technique. Low-temperature photoluminescence measurements were carried out on deformed and reference samples. They showed no detectable contamination with common transition-metal impurity acceptors Cu and Mn after the heat treatment involved in a plastic deformation.

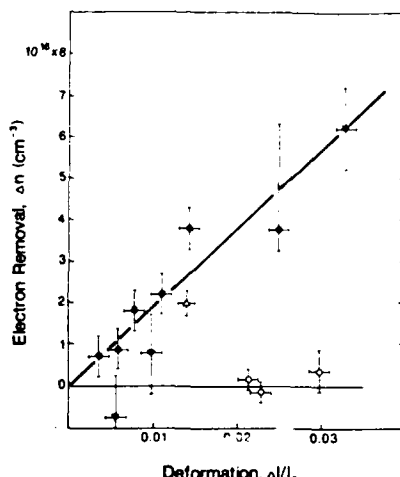


FIG. 1. Electron removal Δn vs the degree of deformation $\Delta l/l_0$. Full circles and full triangles correspond to *n*-type samples deformed along (111) and (110) directions, respectively. Open circles correspond to *p*-type samples deformed in the (111) direction. Open triangle denotes the magnitude of electron removal from EL2 in the (100) direction.

III. RESULTS AND DISCUSSION

A. Free-carrier concentration

Plastic deformation results in a significant decrease of the free-electron concentration n in *n*-type samples; however, it has only a minor effect on the free-carrier concentration in semi-insulating GaAs and practically no effect on the free-hole concentration p in *p*-type GaAs. The net decrease in the majority-carrier concentration determined at 300 K from Hall-effect and conductivity measurements is given in Fig. 1 as a function of the deformation $\Delta l/l_0$.

For *n*-type samples electron concentration decreases linearly with deformation. The same qualitative trend was observed previously for GaAs plastically deformed¹⁴ or irradiated with electrons.²³ It was tentatively interpreted as a result of the creation of new acceptor-type defects. These stress-induced acceptors N_A would compensate shallow donors N_D , causing a decrease in the electron concentration, $n = N_D - N_A$. In addition, the negatively charged, filled acceptors should increase the ionized impurity scattering, leading to a decrease in the electron mobility. Indeed, in deformed samples a large decrease of electron mobility, μ_n , was observed. For example, for $\Delta l/l_0 = 0.014$ the 300-K mobility μ_n dropped to 1900 cm²/V s from 3800 cm²/V s prior to deformation (Table I). According to the GaAs mobility table from Ref. 24, this would correspond to an increase of the total concentration of the ionized centers by about

TABLE I. Effect of plastic deformation on 300-K free-carrier concentration and mobility.

	Before deformation	After deformation	$\Delta l/l_0 (\%)$
n (cm ⁻³)	5.0×10^{16}	3.1×10^{16}	1.5
μ_n (cm ² /V s)	3800 ± 200	1900 ± 200	
p (cm ⁻³)	3.1×10^{16}	3.5×10^{16}	
μ_p (cm ² /V s)	160 ± 40	190 ± 40	2.9

$5 \times 10^{17} \text{ cm}^{-3}$. This concentration appears much too high, and the low mobilities in deformed crystals must result from inhomogeneous distribution of stress-induced scattering centers, and possibly also from the scattering of free carriers by dislocations. The profound effect of macroscale inhomogeneities on the Hall-effect mobility in GaAs was recently demonstrated in Ref. 25. The mobility increase in deformed samples after thermal annealing (which eliminates deformation-induced acceptors) implies that mobility-limiting inhomogeneities are due to nonuniform distribution of stress-induced acceptors.

For *p*-type samples (open circles in Fig. 1) no significant change in hole concentration was observed. This behavior is consistent with the interpretation for *n*-type samples providing that the stress-induced acceptors are sufficiently deep not to be ionized in *p*-type material. From the Fermi energy $E_F - E_v = 0.2 \text{ eV}$ in our samples we conclude that the acceptors must be located at energy exceeding 0.2 eV above the valence band. As electrically neutral these acceptors have no effect on the hole concentration, $p = N_A - N_D$. From the results for *p*-type GaAs we also conclude that no donor-type defects are introduced by plastic deformation in the same energy range ($\gtrsim 0.2 \text{ eV}$ above the valence band). In *p*-type material such donors would be ionized, causing a decrease in the free-hole concentration $\Delta p \approx -\Delta N_D$, in contrast with an experimental observation that $\Delta p = 0$.

Electronic transport in SI GaAs is by far more sensitive to electrical inhomogeneities than that in conducting crystals (due to the lack of free-carrier screening of localized potentials). Accordingly, the deformation-induced changes in electronic characteristics of SI GaAs were determined employing the optical method²⁶ for determination of the Fermi energy and free-carrier concentration from low-temperature measurements of the zero phonon line of the EL2 intracenter absorption.^{27,28} Detailed results are discussed in the subsequent section. We conclude from them that as a result of plastic deformation, the Fermi energy in SI GaAs drops down below the middle of the energy gap. Electron concentration decreases and for a higher degree of deformation the material becomes lightly *p* type. However, in absolute scale Δp and Δn are only of the order of 10^7 cm^{-3} . However, in SI GaAs the deformation-induced acceptors are ionized; they are expected to be compensated by an

increased degree of ionization of the midgap EL2 donor ($\Delta n_{EL2} \approx N_A$) rather than by a change in the free-carrier concentration.

Thus, it is seen that the effects of plastic deformation on the free-carrier concentration are all consistently explained in terms of deformation-induced deep acceptors. They also strongly imply that no donor levels (including the arsenic antisite As_{Ga} defect expected to act as a double donor) are introduced in GaAs by plastic deformation.

B. Deep-level transient spectroscopy

Typical DLTS spectra of deformed and reference samples are presented in Fig. 2. They show EL2 and EL5 electron traps typical for melt-grown GaAs. However, no new electron traps were detected in deformed samples under the same experimental conditions; the DLTS peak heights in deformed samples were larger than in reference samples. Total capacitance values of the diodes were also changed after deformation. Both of these changes were caused by a decrease in the net concentration of ionized centers ($N_D - N_A$). When the correction factors²⁸ for the conversion of DLTS peak heights to the trap concentration were taken into account, the same values of EL2 and EL5 concentrations were found in deformed and reference samples. Identical behavior was observed for all three deformation directions, (100), (110), and (111). An estimated 10% uncertainty in DLTS measurements of EL2 concentration yielded an experimental error $\Delta N_{EL2} \approx \pm 2 \times 10^{15} \text{ cm}^{-3}$. The deformation-induced EL2 concentration changes previously reported for deformed epitaxial layers¹⁴ and horizontal Bridgmann crystals¹⁰ fall within this range. Therefore, one can safely estimate the upper limit for changes in EL2 concentration upon plastic deformation $\Delta l/l_0$ up to 3% to be $\Delta N_{EL2} < 2 \times 10^{15} \text{ cm}^{-3}$. To our knowledge, the results in Ref. 13 (clearly inconsistent with all other published data) are the only exception to this rule.

C. Optical DLTS measurements

Hole traps located in the lower half of the energy gap were studied employing optical DLTS (ODLTS). Optical pulses filling the traps with photoexcited minority carriers were provided by the chopped light from a YAG cw laser. The main limitation of this method is that the light does not fill the traps completely. The equilibrium occupation of the trap in the depletion region under intense illumination is $p_i = N_i \sigma_n / (\sigma_n + \sigma_p)$, where σ_p and σ_n are photoionization cross sections for holes and electrons, respectively. Since $\sigma_n / (\sigma_p + \sigma_n) < 1$, the peak heights in ODLTS spectra underestimate the absolute value of the trap concentration, N_i . However, the peak height can be reliably used to measure a relative change in the concentration of a given trap and to estimate the lower limit of trap concentration.

The typical ODLTS spectra of deformed and reference *n*-type samples are shown in Fig. 3. Both electron and hole traps were observed as positive and negative peaks, respectively. The position of the major electron trap coincides with the EL2 peak in the DLTS spectrum measured at the same gate setting $t_1/t_2 = 20 \text{ ms}/40 \text{ ms}$. The hole trap spectrum for

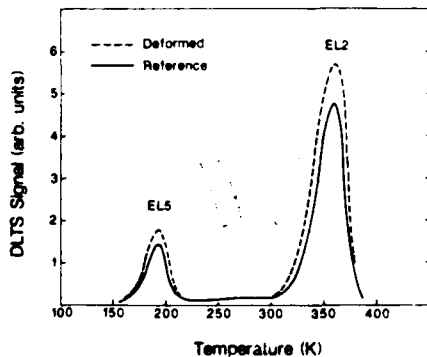


FIG. 2. DLTS spectra corresponding to electron traps in deformed and reference samples of *n*-type GaAs. Gate settings $t_1/t_2 = 20 \text{ ms}/40 \text{ ms}$.

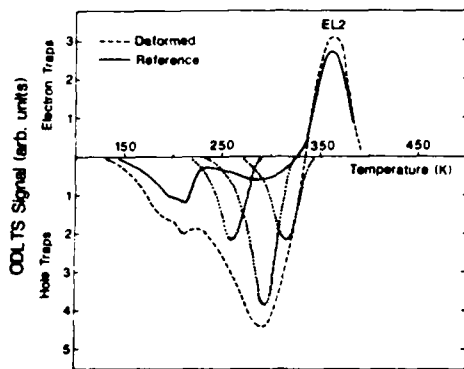


FIG. 3. Optical DLTS spectra in deformed and reference samples of *n*-type GaAs. Components of deconvoluted hole trap ODLTS peak are shown with dotted curves. Gate settings $t_1/t_2 = 20$ ms/40 ms.

the reference sample shows only two bands from 150 to 220 K and between 250 and 330 K, respectively. The spectrum of the deformed crystal is dominated by a large wide band peaked at about 290 K (gate setting 20 and 40 ms). As shown in Fig. 3, the total ODLTS band between 200 and 350 K can be deconvoluted into three components with peaks at 320, 290, and 260 K. The corresponding emission rate activation energy could be estimated only for a dominant 290-K peak. This estimation, $E_A \approx 0.45$ eV, carries a large error of about ± 0.1 eV due to overlapping of the peaks which limits a temperature range useful for construction of individual Arrhenius plots. This trap is similar to the deformation-induced hole trap H_B reported in Ref. 10. The slight difference in DLTS peak position is due to a different gate setting ($t_1/t_2 = 1.95$ ms/7.8 ms) used in Ref. 10.

As shown in Fig. 4, the concentration of this trap increases linearly with deformation. As pointed out above, ODLTS does not give the absolute value of the trap concentration, but only its lower limit. For the 0.45-eV trap this limit is about $1 \times 10^{16} \text{ cm}^{-3}$ for $\Delta l/l_0 = 2\%$. A similar estimation for the combined concentration of other deformation-induced traps (i.e., the components of the deconvoluted spectrum in Fig. 3) yields the value $> 1.5 \times 10^{16} \text{ cm}^{-3}$. Total hole trap concentration $\gtrsim 2.5 \times 10^{16} \text{ cm}^{-3}$ at $\Delta l/l_0 = 2\%$ is in good agreement with the total acceptor concentration $N_A \approx 4 \times 10^{16} \text{ cm}^{-3}$ required to account for the electron removal data shown in Fig. 1.

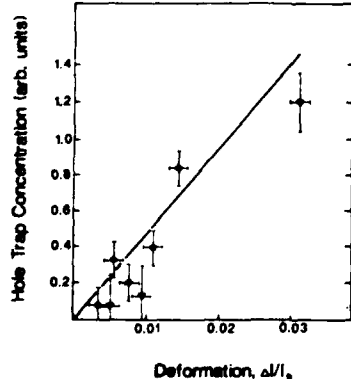


FIG. 4. Concentration of the dominant deformation-induced hole trap (ODLTS peak at about 290 K) vs the deformation $\Delta l/l_0$.

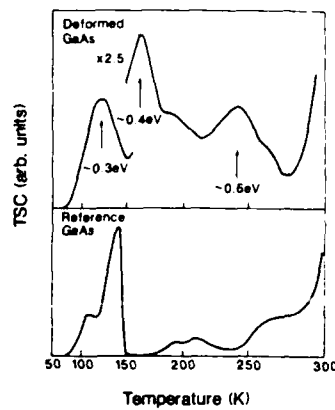


FIG. 5. Thermally stimulated current spectra of deformed (upper spectrum) and reference (lower spectrum) samples of SI GaAs

D. Thermally stimulated current

The thermally stimulated current (TSC) method is especially useful for the study of electron and hole traps in high-resistivity materials²⁹ where standard DLTS and capacitance ODLTS are not readily applicable. The method employs optical excitation of excess carriers at low temperature. Subsequent continuous temperature increase in the dark leads to a release of carriers from traps and creates peaks of the electric current versus temperature.

TSC spectra of the deformed and reference samples are shown in Fig. 5. The presence of three new deformation-induced traps is evidenced by TSC peaks at 125, 160, and 240 K. These temperatures correspond roughly to trap energies of 0.3, 0.4, and 0.6 eV,²⁹ which is in good agreement with hole traps observed by the optical DLTS in deformed samples of *n*-type GaAs.

E. Optical absorption

Optical absorption spectra measured at 77 K on *n*-type GaAs samples undeformed and plastically deformed to different $\Delta l/l_0$ values are shown in Fig. 6. The spectrum of the reference sample is a typical EL2-related absorption observed in the melt-grown GaAs.^{27,28,30} The near-infrared part of this spectrum originates from EL2 photoionization with the onset at about 0.8 eV. Intracenter EL2 transitions (shadowed area) for $1.0 < h\nu < 1.3$ eV superimposed on the photoionization background produce an absorption bulge around 1.2 eV. It is evident from Fig. 6 that the plastic defor-

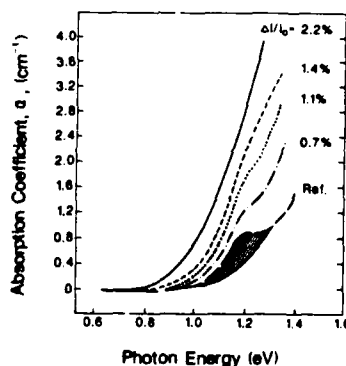


FIG. 6. 77-K optical absorption spectra of *n*-type GaAs for different deformation $\Delta l/l_0$. Dashed area on the spectrum of undeformed reference samples denotes the EL2 intracenter absorption

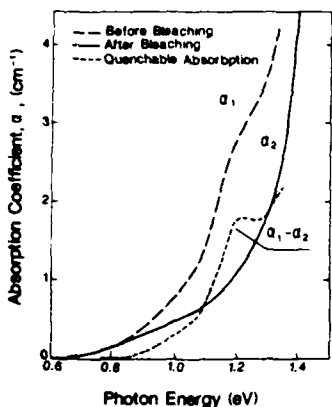


FIG. 7. Low-temperature (6 K) optical absorption spectra of *n*-type GaAs deformed to $\Delta l/l_0 = 2.2\%$.

mation significantly changes an overall shape of the absorption spectrum, introducing a featureless absorption background which increases monotonically toward the energy gap. The EL2 contribution to absorption in deformed samples can still be separated using optical quenching at low temperature which transfers the EL2 into an optically inactive metastable state. The quenchable absorption (i.e., $\alpha_1 - \alpha_2$, in Fig. 7) corresponds to EL2 while the unquenchable part (α_2 in Fig. 7) corresponds to other absorption processes. Employing optical quenching by a strong white light illumination for 10 min at 6 K we have found that for all plastically deformed *n*-type samples, the spectral shape and the intensity of the quenchable part ($\alpha_1 - \alpha_2$) were the same as that for the reference sample. The monotonically increasing (with $h\nu$) absorption component (α_2 in Fig. 7) became clearly visible after quenching of the absorption.

The magnitude of quenchable absorption and total absorption change $\Delta\alpha = \alpha(1.2 \text{ eV}) - \alpha(0.7 \text{ eV})$ are shown in Fig. 8. The quenchable absorption remains constant over the entire deformation range. However, the total absorption change, $\Delta\alpha$, increases linearly with the deformation $\Delta l/l_0$. Without spectral measurements combined with optical quenching, the increase of $\Delta\alpha$ could easily be taken as apparent proof of the increase in EL2 concentration. [Note that it is a standard practice in GaAs to assume that the entire sub-band-gap absorption originates from EL2. Thus, the difference in absorption for two photon energies $\Delta\alpha = \alpha(1.2 \text{ eV}) - \alpha(0.7 \text{ eV})$ is treated as a measure of the

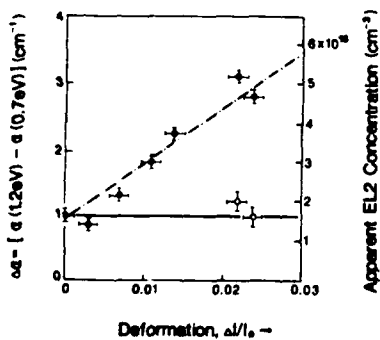


FIG. 8. Deformation-induced change in the absorption coefficient; total change, dark circle and broken line; EL2-related quenchable absorption, light circles and solid line. Measurements at 6 K.

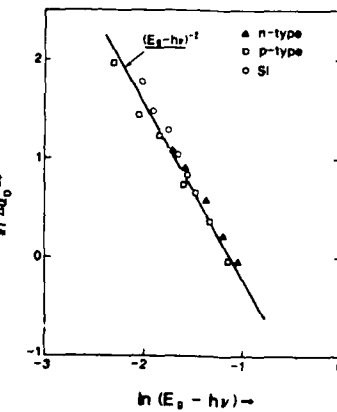


FIG. 9. Energy dependence of the deformation-induced unquenchable change in the optical absorption coefficient. Points, experimental; line, theoretical dependence for optical absorption due to dislocations.

EL2 concentration.] In fact, the deformation-induced absorption change has nothing to do with either EL2 or any other localized deep level. First of all, the same unquenchable absorption was observed in deformed samples—*n* type, semi-insulating, and *p* type, i.e., irrespective of the Fermi energy shift from the bottom of the conduction band to the top of the valence band. It is very unlikely that the spectral shape and the intensity of any photoionization in GaAs could remain the same when the level involved undergoes a change from occupied to empty. Secondly, as shown in Fig. 9, the deformation-induced absorption satisfies a specific spectral dependence $\Delta\alpha_D = K \times (E_g - h\nu)^{-2}$, incompatible with standard deep-level transitions.³¹ However, this dependence was previously observed in plastically deformed direct band-gap semiconductors (GaAs and CdSe) and was explained in terms of a deformation potential model which considered a decrease in the energy gap E_g in the stress field of dislocations.³²

F. 1.038-eV zero phonon line

Low-temperature high-resolution measurements of optical absorption have shown that the plastic deformation changes the shape and the intensity of the characteristic 1.039-eV zero phonon line (ZPL) located at the onset of the EL2 intracenter transition.²⁷ The results presented in Fig. 10 were obtained with semi-insulating GaAs deformed in the (100) direction with $\Delta l/l_0 = 0.013$. With respect to the undeformed sample the peak position is shifted to a slightly higher energy. In addition, the line broadens and it can be deconvoluted into three components. This behavior is consistent with the splitting pattern of the line under applied stress.³³ Thus, for the stress applied in the (100) direction

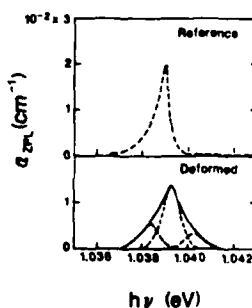


FIG. 10. High-resolution 6-K spectra of the zero phonon line of the EL2 intracenter absorption in SI GaAs. Upper spectrum, before deformation; lower spectrum, after deformation to $\Delta l/l_0 = 1.4\%$.

one expects a slight shift of the line to higher energy resulting from two unresolvable line components moving upwards in energy. The additional two components must result from stresses in the (111) and (110) directions (both of which split the line into high- and low-energy components) associated with the not exactly uniaxial character of plastic deformation. Residual stresses present in the sample after deformation may be associated with stress fields around dislocations discussed in conjunction with a deformation-induced optical absorption tail.

It should be noted that the presently observed behavior of the zero phonon line may account for an apparent complex character of the line in some of the crystals in terms of the stress-induced effects.

In *n*-type GaAs the broadening of ZPL is the only stress-induced effect. However, in semi-insulating crystals an additional phenomenon is observed which proves the importance of the deformation-induced shift of the Fermi energy. As discussed in detail elsewhere,²⁶ the liquid-He measurements of the zero phonon line in GaAs directly after cooling, α_{ZPL}^1 , and after optical bleaching followed by 10-min annealing at 140 K, α_{ZPL}^2 , yield the EL2 occupancy fraction $\eta = \alpha_{ZPL}^1 / \alpha_{ZPL}^2$. (This approach is based on the fact that the ZPL measures the concentration of occupied EL2 and that the complete transition to a metastable state leaves all EL2 in an occupied state.) As shown in Table II, the EL2 occupancy fraction in reference crystal is $\eta = 0.95$, while after plastic deformation it drops down to about 0.45. The increase in ionized EL2 concentration, ΔN_{EL2} , must be equal to a net concentration of the ionized acceptors ΔN_A introduced by a deformation. The experimental point marked in Fig. 1 with an open triangle corresponds to this value.

It is of importance to note that the presently proven downward shift of the Fermi energy in deformed SI GaAs (caused by deformation-induced acceptors in the lower half of the energy gap) provides a missing link in explanation of the apparently conflicting findings: i.e., the lack of increase of the EL2 concentration and an increase in EPR signal of an ionized antisite defect As_{Ga} clearly related to EL2.^{17,21,22} It is now evident that an increase of EPR signal results from an increase in the fraction of ionized As_{Ga} defects rather than the increase of the total antisite concentration.

G. Annealing

Plastically deformed samples, after characterization, were annealed at several temperatures between 600 and 900 °C. The annealing was performed in a closed quartz ampul with a controlled arsenic pressure, corresponding to equilibrium conditions. After annealing the samples were repolished and characterized again.

We found that prolonged annealing at 800 or 850 °C eliminated all deformation-induced changes in electrical properties. The most important effect of annealing was perhaps the total disappearance of the 0.45-eV hole trap. The ODLTS spectrum of the deformed and subsequently annealed sample (10 h at 850 °C) was virtually identical to the reference sample shown in Fig. 2(b). According to the discussion in Sec. III A and III B, this acceptor clearly contributes to free-electron removal and possibly also to a decrease in electron mobility. In fact, after annealing, the carrier concentration and the mobility recovered to their predeformation values.

DLTS and optical absorption measurements have led to a new observation of a decrease in the EL2 concentration during annealing of deformed samples. Figure 11 presents the results of optical absorption measurements on deformed and annealed samples. All spectra show a consistent trend, namely, the EL2 absorption band steadily decreases with increasing deformation $\Delta l/l_0$. For samples deformed by 1.4%, only half of the original EL2 absorption is preserved. The samples used in those measurements were all *n* type after annealing with carrier concentration in the 10^{16}-cm^{-3} range. Therefore, all EL2 centers were filled with electrons, and consequently the decrease of the absorption band was a direct measure of the decrease in the EL2 concentration.

Similar results were also obtained with DLTS. They are summarized in Fig. 12 together with the results from optical measurements. It is clear that although deformation itself does not change the EL2 concentration, subsequent annealing of deformed samples leads to partial EL2 annihilation. Because in undeformed samples the EL2 defect was stable up to 900 °C, this annihilation must result from the interaction of EL2 with stress-induced defects, dislocations, and/or native defects. The exact nature of this interaction is not known at present.

IV. SUMMARY AND CONCLUSIONS

The introduction of deep acceptors is the most important primary effect which is responsible for most of the deformation-induced changes in electronic properties of GaAs. In *n*-type GaAs the acceptors are ionized. They compensate shallow donors causing the free-electron removal. The presence of ionized acceptors decreases the electron mobility value due in part to increased ionized impurity scattering and in part to inhomogeneities associated with nonuniform distribution of the acceptors. As long as the deformed GaAs remains conducting *n* type, the midgap EL2 donor is completely occupied. Accordingly, no change in the characteristic quenchable EL2 absorption band is observed after deformation of *n*-type GaAs. However, the deformation

TABLE II. Effect of deformation on EL2 occupation in SI GaAs deduced from the zero phonon line absorption.

Sample	Deformation $\Delta l/l_0$ (%)	EL2 occupancy fraction $\eta = \alpha_{ZPL}^1 / \alpha_{ZPL}^2$	Fraction of EL2 ionized ($1 - \eta$)	Net concentration of ionized acceptors (cm^{-3})
As-grown	0	0.95	0.05	2.0×10^{15}
Deformed	1.4	0.45	0.55	2.0×10^{16}

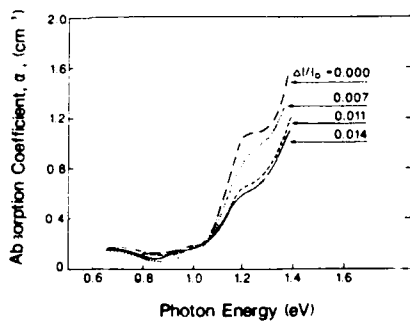


FIG. 11. 77-K optical absorption spectra of deformed *n*-type samples annealed at 850 °C for 10 h.

produces a featureless unquenchable absorption tail $\Delta\alpha_D$, which extends well into the subband-gap region. In Refs. 17 and 21 this absorption tail was considered to be due to transitions via localized levels of the arsenic antisite As_{Ga} defect introduced by deformation. We found no evidence supporting this interpretation. On the contrary, the characteristic spectral dependence $\Delta\alpha_D \sim (E_g - h\nu)^{-2}$ is consistent with "the dislocation absorption" which is due to energy gap changes in the stress field of dislocations.

In *p*-type GaAs the deformation causes no change in the concentration of free holes and had no effect on the free-carrier mobility. Results obtained with *p*-type GaAs also prove that no donors are produced by plastic deformation at energies higher than 0.2 eV above the valence band. This conclusion received further support from DLTS data which showed no new electron traps and no appreciable change in concentration of any electron traps present prior to the deformation. Therefore, we must reject the hypothesis of Refs. 17 and 21 that the donor-type arsenic antisite defect As_{Ga} is created during the plastic deformation. For similar reasons, we also reject the hypothesis of Refs. 18 and 19 of the creation of the arsenic interstitial As_I donor with energy level about 0.77 eV below the conduction band. Both of these hypotheses were postulated to explain the increase in the EPR quadruplet signal in plastically deformed GaAs. Present results fully support the very recent explanation of this effect by Bray in Ref. 22 in terms of the increased ionization of As_{Ga} brought about by the compensating action of the deformation-induced acceptors. Our measurement of the

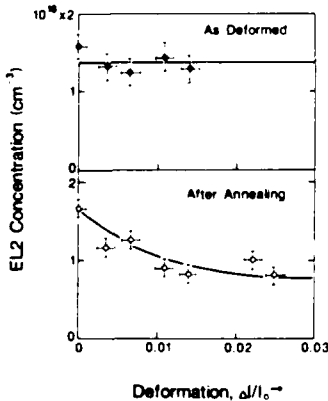


FIG. 12. EL2 concentration vs the degree of deformation $\Delta l/l_0$ for as-deformed samples (upper figure) and after 850 °C annealing for 10 h (lower figure).

zero phonon line in SI GaAs provided the first direct evidence of the increased ionization of the midgap donor EL2 (related to the antisite defect As_{Ga}) in deformed crystals.

Thermal annealing experiments showed that the deformation-induced acceptors fully anneal out at temperatures of about 800 °C. However, the annealing also takes place at lower temperatures > 600 °C. The EL2 concentration in deformed samples was found to decrease during annealing. The unique mechanism of this process cannot be formulated at present. We are also unable to identify the origin of the native acceptors induced by deformation. However, it is possible that the EL2 annihilation may result from the interaction of As_{Ga} with native defects containing a gallium vacancy. An acceptor-type gallium vacancy may also be a constituent of defects responsible for the deformation-induced native acceptors. Further studies are obviously needed to identify the pertinent defects and their interaction.

ACKNOWLEDGMENTS

The authors are grateful to Dr. W. Walukiewicz for valuable discussions. They are also grateful to the U.S. Air Force Office of Scientific Research and to Sumitomo Electric Industries, Ltd. for financial support.

- ¹A. S. Jordan, R. Caruso, A. R. Von Neida, and J. W. Nielsen, *J. Appl. Phys.* **52**, 3331 (1981).
- ²A. S. Jordan, A. R. Von Neida, and R. Caruso, *J. Cryst. Growth* **70**, 555 (1984).
- ³A. S. Jordan, R. Caruso, and A. R. Von Neida, *Bell Syst. Tech. J.* **59**, 593 (1980).
- ⁴T. Obokata, T. Matsumura, K. Terashima, F. Orito, T. Kikuta, and T. Fukuda, *Jpn. J. Appl. Phys.* **23**, L602 (1984).
- ⁵M. R. Brozel, I. Grant, R. M. Ware, and D. J. Stirland, *Appl. Phys. Lett.* **42**, 610 (1983).
- ⁶D. E. Holmes and R. T. Chen, *J. Appl. Phys.* **55**, 3588 (1984).
- ⁷Y. Matsumoto and H. Watanabe, *Jpn. J. Appl. Phys.* **21**, L515 (1982).
- ⁸S. Miyazawa, T. Mizutani, and H. Yamazaki, *Jpn. J. Appl. Phys.* **21**, L542 (1982).
- ⁹Y. Nanishi, S. Ishida, T. Honda, H. Yamazaki, and S. Miyazawa, *Jpn. J. Appl. Phys.* **21**, L335 (1982).
- ¹⁰T. Isida, K. Maeda, and S. Takeuchi, *Appl. Phys.* **21**, 257 (1980).
- ¹¹T. Wosinski, *Phys. Status Solidi A* **60**, K149 (1980).
- ¹²W. E. Weber, H. Ennen, U. Kaufman, J. Windscheif, J. Scheider, and T. Wosinski, *J. Appl. Phys.* **53**, 6140 (1982).
- ¹³T. Wosinski, A. Morawski, and T. Figiel, *Appl. Phys. A* **30**, 233 (1983).
- ¹⁴F. Hasegawa, N. Yamamoto, and Y. Nannichi, Extended Abstracts of the 16th Conference on Solid State Devices and Materials, Kobe, Japan, 1984, p. 169.
- ¹⁵S. Benakki, A. Goltzene, C. Schwab, Wang Guangyu, and Zou Yuanxi, *Phys. Status Solidi B* **138**, 143 (1986).
- ¹⁶D. Gerthsen, *Phys. Status Solidi A* **97**, 527 (1986).
- ¹⁷E. R. Weber, in *Semi-insulating III-V Materials*, edited by D. C. Look and J. S. Blakemore (Shiva, Nantwich, England, 1984), p. 296.
- ¹⁸K. Sumino, in *Defects and Properties of Semiconductors*, edited by J. Chikawa, K. Sumino, and K. Wada (KTK Scientific, Tokyo, Japan, 1987), Chap. 1.
- ¹⁹M. Suezawa and K. Sumino, *Jpn. J. Appl. Phys.* **25**, 533 (1986).
- ²⁰L. Samuelson, P. Omling, E. R. Weber, and H. G. Grimmeis, in *Semi-insulating III-V Materials*, edited by D. C. Look and J. S. Blakemore (Shiva, Nantwich, England, 1984), p. 268.
- ²¹P. Omling, E. R. Weber, and L. Samuelson, *Phys. Rev. B* **33**, 5880 (1986).
- ²²R. Bray, *Solid State Commun.* **60**, 867 (1986); E. R. Weber, *Solid State Commun.* **60**, 871 (1986).
- ²³F. Yamaguchi and C. Ventura, *J. Appl. Phys.* **57**, 604 (1985).
- ²⁴W. Walukiewicz, J. Lagowski, L. Jastrzebski, M. Lichtensteiger, and H. C. Gatos, *J. Appl. Phys.* **50**, 899 (1979).

- ²⁵W. Walukiewicz, Le Wang, L. M. Pawlowicz, J. Lagowski, and H. C. Gatos, *J. Appl. Phys.* **59**, 3144 (1986).
- ²⁶J. Lagowski, M. Bugajski, M. Matsui, and H. C. Gatos, *Appl. Phys. Lett.* **51**, 511 (1987).
- ²⁷M. Kaminska, M. Skowronski, J. Lagowski, J. M. Parsey, and H. C. Gatos, *Appl. Phys. Lett.* **43**, 302 (1983).
- ²⁸M. Skowronski, J. Lagowski, and H. C. Gatos, *J. Appl. Phys.* **59**, 2451 (1986).
- ²⁹G. M. Martin, in *Semi-Insulating III-V Materials*, edited by G. J. Rees (Shiva, Orpington, UK, 1980), p. 13, and references therein.
- ³⁰G. M. Martin, *Appl. Phys. Lett.* **39**, 747 (1981).
- ³¹G. Lucovsky, *Solid State Commun.* **3**, 209 (1965).
- ³²A. V. Bazhenov and L. I. Krashil'nikova, *Sov. Phys. Solid State* **26**, 356 (1984).
- ³³M. Kaminska, M. Skowronski, and W. Kuszko, *Phys. Rev. Lett.* **55**, 2204 (1985).